

Solutions of the Ginzburg-Landau Equation of Interest in Shear Flow Transition

By Michael J. Landman

The Ginzburg-Landau equation may be used to describe the weakly nonlinear 2-dimensional evolution of a disturbance in plane Poiseuille flow at Reynolds number near critical. We consider a class of quasisteady solutions of this equation whose spatial variation may be periodic, quasiperiodic, or solitary-wave-like. Of particular interest are solutions describing a transition from the laminar solution to finite amplitude states. The existence of these solutions suggests the existence of a similar class of solutions in the Navier-Stokes equations, describing pulses and fronts of instability in the flow.

1. Introduction

The amplitude equation derived by Stewartson and Stuart [22] for 2-dimensional disturbances to plane Poiseuille flow at Reynolds numbers close to the critical Reynolds number Re_c of linear instability is of the form

$$\frac{\partial A}{\partial t} = a \frac{\partial^2 A}{\partial x^2} + (Re - Re_c) A + dA|A|^2. \quad (1.1)$$

This equation, whose coefficients a and d are complex, has become widely known in the literature as the (generalized) Ginzburg-Landau (GL) equation and has been studied in a variety of contexts. For a list of references see [13]. In the context of plane Poiseuille flow, which can be regarded as a prototype for other

Address for correspondence: Dr. Michael J. Landman, Department of Applied Mathematics, California Institute of Technology 217-50, Pasadena, CA 91125.

parallel shear flows, A describes the amplitude of the envelope modulating the marginally stable Tollmien-Schlichting (TS) waves [4] given by linear theory, as viewed in the reference frame of the group velocity.

Most investigators have concentrated on the case when the real part of the coefficient of the nonlinear term, d_+ , is negative. A negative value of d_+ arises when the GL equation is derived as the amplitude equation describing a supercritical bifurcation as in convection problems [17]. In this case the GL equation has been shown to exhibit a large variety of behaviors, including chaotic behavior both temporally [16, 13] and spatially [2, 10, 11].

For 2-dimensional plane Poiseuille flow and other systems with a subcritical bifurcation, d_+ is positive however, in which case the GL equation has quite different behavior. The analysis in the literature for this case is chiefly concerned with seeking time dependent singularities of solutions of (1.1); however, Hocking and Stewartson's [8] analysis and numerical studies failed to find singular bursts in finite time for the Poiseuille parameters.

This paper is concerned with the structure of solutions of Equation (1.1) with the simple time dependence

$$A = e^{-i\Omega t} \Phi(x - ct). \quad (1.2)$$

We shall call solutions of this form quasisteady, where the function Φ satisfies a second order complex ordinary differential equation of the form of a damped Duffing equation. We concentrate on studying this equation for the coefficient values applicable to 2-dimensional plane Poiseuille flow.

Solutions of the form (1.2) with $c = 0$ have been studied by several authors for the GL equation with d_+ negative [21, 10]. These studies have primarily concentrated on a single branch of spatially periodic solutions [$\Phi(x) = \Phi(x + L)$] which bifurcates supercritically from the nontrivial stable uniform solution of (1.1) as an appropriate parameter is varied. P. Holmes [12] has also studied quasisteady solutions with $c = 0$ for the perturbed nonlinear Schrödinger equation, which is of the form of the GL equation.

We have found a large class of solutions of the form (1.2) for the GL equation with d_+ positive which are applicable to plane Poiseuille flow.

A previously known subset of solutions is those of the plane waves

$$A = Be^{i(kx - \Omega t)}. \quad (1.3)$$

These correspond to the well-known finite amplitude travelling wave solutions of the full fluid equations for flow between parallel plates. Bifurcations from the plane wave solutions (1.3) and the trivial solution have recently been discussed by C. Holmes [11] using center manifold theory.

We have been able to find other spatially periodic and quasiperiodic solutions of the GL equation. When $Re > Re_c$ a third branch of periodic envelope solutions bifurcates from the Orr-Sommerfeld neutral curve in addition to the pair of plane wave solutions. This new family of solutions has amplitude greater than the amplitude B of the solutions (1.3). When $Re < Re_c$ other periodic solutions are

found to exist for d , positive which are analogous to those studied by other investigators for d , negative. We continued these branches numerically in the parameters Ω and c , and find a complex structure of other spatially periodic and quasiperiodic solutions bifurcating from them. These solutions all describe slow spatial modulations to the neutrally stable TS waves.

A wide variety of solitary wave solutions also exist, some of which were previously known, that connect the physically attainable states of the plane waves and the zero amplitude laminar state. These solutions can be of breather type, decaying at plus and minus infinity; frontlike, describing a transition from disturbed to laminar flow; or holelike, describing localized modulations of the plane wave state. Other more general transitions from the laminar or plane wave states to spatially quasiperiodic or perhaps chaotic states have also been found numerically.

The remainder of this introduction briefly describes how the GL equation is derived for Poiseuille flow. We then consider in Section 2 a complex second order ordinary differential equation of the form of a complex damped Duffing equation, which arises in the study of quasisteady solutions of the form (1.2). This 4-dimensional dynamical system may in some instances be reduced to a 3-dimensional first order system, which is similar to systems recently discussed by other authors but in different parameter regimes. We analyze the stability and bifurcation structure of the 4- and 3-dimensional systems in Sections 3 and 4 which is preliminary to our numerical investigations which follow. Section 5 describes some of the complex structure of spatially periodic and quasiperiodic solutions for both the 4- and 3-dimensional equations. A more detailed discussion of this class of quasisteady solutions is given in [15]. Section 6 investigates the possible quasisteady solitary wave solutions of the GL equation, with a description of the previously known exact solutions in the setting of the 3-dimensional equations. A numerical search reveals a far larger class of solitary waves and their generalization to other transitions from the trivial and plane wave solutions.

Real shear flow instability is of course fully 3-dimensional in space and is often found to occur well below the critical Reynolds number of linear theory. In accordance with this, numerical evidence suggests that the quasisteady solutions of the GL equation for Poiseuille flow are unstable. Nevertheless, corresponding branches of solutions may exist for the Navier-Stokes equations for Poiseuille flow which stabilize at finite amplitude and lower Re than the critical Re_c of 5772. This scenario is in fact true for the continuation of the plane wave solutions in the space of 2-dimensional Navier-Stokes solutions. It is thus our belief that the Stewartson-Stuart weakly nonlinear theory may give rise to solutions which are present in the full Navier-Stokes equations which may be relevant to the process of transition. This conjecture will be further discussed in the last section of this paper.

1.1. The derivation of the GL equation for 2-D plane Poiseuille flow

In parallel shear flow the GL equation arises by considering the evolution of a 2-D disturbance to steady laminar viscous flow between two horizontal plates driven by a constant pressure gradient or fluid flux. We take x in the streamwise

direction and y in the vertical direction, where all variables are nondimensionalized with respect to the channel half width and maximum velocity of the parabolic base flow. The boundary conditions imposed are those of constant flux and no slip at the walls.

Following Stewartson and Stuart [22], who use the method of multiple scales, the stream function ψ is expanded about the parabolic base flow, both in a power series in the small parameter ϵ (proportional to amplitude of the modulation) and in a harmonic series of the most unstable wave (the Tollmien-Schlichting wave given by linear theory). The lowest order term which describes modulations to the neutrally stable wave is given by

$$\psi - y(1 - \frac{1}{3}y^2) = \epsilon \hat{A}(\xi, \tau) \phi(y) e^{i\alpha_c(x - c_{cr}t)} + \text{c.c.} + O(\epsilon^2), \quad (1.4)$$

where ξ and τ are the scaled slow streamwise coordinate and slow time given by

$$\xi = \epsilon(x - c_g t), \quad \tau = \epsilon^2 t.$$

c_g is the group velocity at which the energy of the modulation propagates according to linear theory, and $\phi(y)$ is the first Orr-Sommerfeld eigenfunction at the nose of the Orr-Sommerfeld neutral stability curve where $\text{Re} = \text{Re}_c$ [4]. In this way ϵ may also be thought of as being related to the inverse length and time scales of the disturbance.

The Reynolds number is found to scale with ϵ^2 , and we write

$$s_r(\text{Re} - \text{Re}_c) = \epsilon^2 \sigma_r, \quad (1.5)$$

where s_r is a fixed positive constant given below and is included for consistency with Stewartson and Stuart. In their original derivation they chose to scale $|\sigma_r| = 1$, whereas we consider σ_r as an order one parameter determining the Reynolds number. We find that this approach has the advantage that the structure of solutions either side of critical can be studied without the necessity for ϵ and thus the amplitude to go through zero.

All of the constants above may be calculated from the linear dispersion relation (i.e., the Orr-Sommerfeld neutral stability curve), and from [1] these are given by

$$\text{Re}_c = 5772.2, \quad c_{cr} = 0.264, \quad \alpha_c = 1.02,$$

$$s_r = 0.168 \times 10^{-5}, \quad c_g = 0.383.$$

The GL equation for \hat{A} is derived by substituting the expansion (1.4), including higher order corrections to the base flow and harmonics of the TS wave, into the Navier-Stokes equations. At order $O(\epsilon^3)$ a solvability condition

must be satisfied for the inhomogeneous equation, and the GL equation

$$\frac{\partial \hat{A}}{\partial \tau} = b \frac{\partial^2 \hat{A}}{\partial \xi^2} + \frac{s}{s_r} \sigma_r \hat{A} + \kappa \hat{A} |\hat{A}|^2 \quad (1.6)$$

results.

The coefficients relevant to Poiseuille flow have been calculated numerically, and we quote these values from [1] as

$$b = 0.187 + 0.0275i, \quad \kappa = 30.8 - 173i, \quad s = (0.168 + 0.811i) \times 10^{-5}. \quad (1.7)$$

On rescaling \hat{A} to A and ξ to x (distinct from the fast scale x) in (1.6) such that

$$A = \sqrt{|\kappa_r|} \exp\left(-\frac{i\sigma_r s_i \tau}{s_r}\right) \hat{A}, \quad x = \frac{\xi}{\sqrt{b_r}},$$

we are able to scale the magnitudes of the real parts of b and κ to unity and make the coefficient of the linear term real. We then get the normal form of the GL equation,

$$\frac{\partial A}{\partial t} = (a_r + ia_i) \frac{\partial^2 A}{\partial x^2} + \sigma_r A + (d_r + id_i) A |A|^2, \quad (1.8)$$

where we have also replaced the slow variable τ with t for convenience of notation. Note that $a_r \geq 0$ is necessary for well-posedness, and we shall assume this condition throughout. From the relevant values (1.7) the coefficients in Equation (1.8) become

$$\begin{aligned} a_r &= 1, & d_r &= 1, \\ a_i &= 0.147, & d_i &= -5.62. \end{aligned} \quad (1.9)$$

These coefficients are thus determined solely by the physics, and in what follows we shall use their values to guide the parameter ranges in which we are interested. Although the above scaling can always be performed provided $b, \kappa \neq 0$, in general we shall retain a , and d , in our analysis, but use the values (1.9) in our numerical calculations. We shall also find it useful to define the quantities

$$a_0 \equiv \frac{a_i}{a_r}, \quad d_0 \equiv \frac{d_i}{d_r}.$$

2. Quasisteady solutions

2.1. Plane wave solutions

The simplest and best-known exact solutions for the GL equation (1.8) are those of constant amplitude plane waves

$$A = Be^{i(kx - \Omega t)}, \quad (2.1)$$

where

$$|B| = \sqrt{\frac{a_r k^2 - \sigma_r}{d_r}}, \quad \Omega = (a_i - d_0 a_r)k^2 + d_0 \sigma_r,$$

and the phase of B is arbitrary. For the Poiseuille coefficients, if $\sigma_r < 0$ ($\text{Re} < \text{Re}_c$), these wavetrain solutions exist for all wavenumbers k and have amplitude bounded above zero. When $\sigma_r > 0$ ($\text{Re} > \text{Re}_c$), we require $k^2 > \sigma_r/a_r$. For a given σ_r and wavenumber a pair of plane waves exists; the solution with wavenumber $k > 0$ we call T_+ , the other with wavenumber $k < 0$ we call T_- .

These wave solutions describe for asymptotically small amplitude the 2-D finite amplitude periodic traveling wave solutions that bifurcate from the Orr-Sommerfeld curve for the linear stability of Poiseuille flow. These finite amplitude waves are of the form

$$\psi = F(x - c_p t, y, \text{Re}, \alpha),$$

where F is of period $2\pi/\alpha$ in the first variable and satisfies no slip boundary conditions in y . See Figure 1. c_p is then determined by a nonlinear dispersion relation for a range of Re and α . These equilibrium states have been studied by several investigators [23, 6] and are found to lie on a surface in $(\text{Re}, \alpha, \text{amplitude})$ space which exists down to Reynolds numbers of about 2500. The surface is doubled valued in amplitude, and the upper branch is stable to 2-D superharmonic disturbances.

Note that by allowing σ_r to be an order one parameter we can see that a family of plane waves of equal amplitude exists in a neighborhood of the “nose” of the Orr-Sommerfeld curve on the locus $\sigma_r = a_r k^2 + \text{const}$ which gives a relation between the Reynolds number and the wavenumber for these waves.

2.2. The complex damped Duffing equation and related dynamical systems

More generally we can seek solutions to the GL equation (1.8) of the form

$$A = e^{-i\Omega t} \Phi(x - ct), \quad (2.2)$$

where the wave speed c provides an order ϵ correction to the group velocity of linear theory if we go back to the derivation of A from the stream function. The modulus of the complex amplitude is therefore steady in a frame of velocity $c_g + \epsilon c$. Substitution of (2.2) into the GL equation (1.8) gives the ordinary

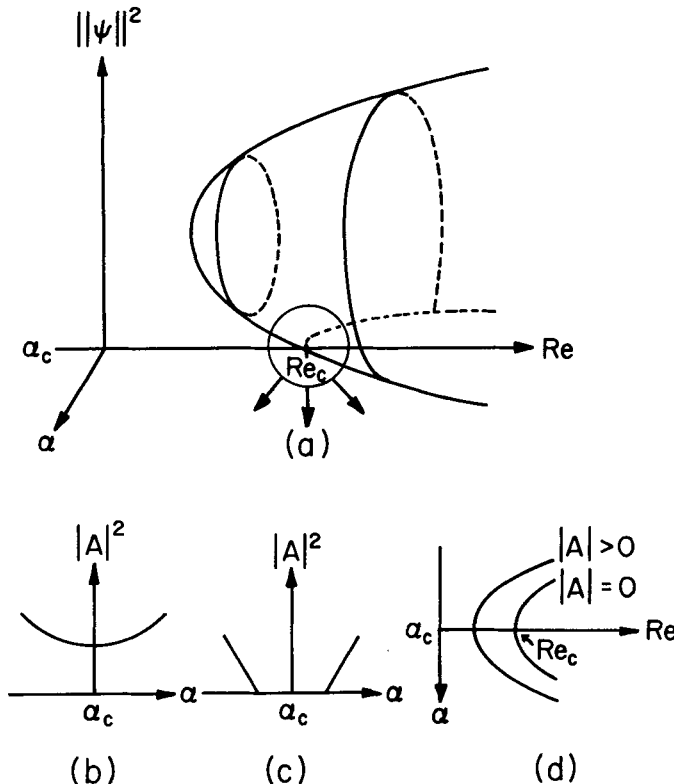


Figure 1. (a) Energy surface of 2-dimensional finite amplitude traveling waves for Poiseuille flow, as a function of Reynolds number and wavenumber. (b)–(d): Small amplitude approximation given by the GL plane waves. $\sigma_r < 0$ in (b), and $\sigma_r > 0$ in (c).

differential equation for $\Phi(X)$ as a function of $X = x - ct$:

$$(a_r + ia_i)\Phi'' + c\Phi' + (\sigma_r + i\Omega)\Phi + (d_r + id_i)\Phi|\Phi|^2 = 0.$$

It is convenient to rewrite this equation as

$$\Phi'' + (c_1 + ic_2)\Phi' + (\delta_1 + i\beta)\Phi = (\delta_2 + i\gamma)\Phi|\Phi|^2, \quad (2.3)$$

where from the Poiseuille coefficients (1.9)

$$\begin{aligned} \beta &= \frac{a_r\Omega - a_i\sigma_r}{|a|^2}, & \gamma &= \frac{a_id_r - a_rd_i}{|a|^2} = 5.65, \\ \delta_1 &= \frac{a_r\sigma_r + a_i\Omega}{|a|^2}, & \delta_2 &= -\frac{a_rd_r + a_id_i}{|a|^2} = -0.170, \\ c_1 &= \frac{ca_r}{|a|^2}, & c_2 &= -\frac{ca_i}{|a|^2}. \end{aligned} \quad (2.4)$$

Equation (2.3) is a complex version of the damped Duffing equation. This equation has been studied in the undamped case ($c = 0$) by Sirovich and Newton [21], C. Holmes and Wood [10], and P. Holmes [12], although in different parameter regimes than the one in which we are interested.

The six parameters above are of course not all independent, and they may be reduced in number by rescaling at most two of them. We have sometimes found it convenient to scale the magnitudes of δ_1 and δ_2 to unity, by scaling amplitude and space. In so doing four cases of the complex Duffing equation arise, depending on the signs of δ_1 and δ_2 . In general we will remain with the parameters (2.4), however, noting that varying Ω is equivalent in scaled parameters to varying β and fixing δ_1 .

The equation (2.3) describes the spatial behavior of quasisteady solutions (2.2) of the GL equation and is the equation on which this study will concentrate. Notice there are two undetermined parameters Ω and c , the temporal frequency of oscillation and the group velocity correction respectively. The coefficients γ and δ_2 in the complex damped Duffing equation are regarded as being determined by the physics of the problem. $c_1 = -c_2/a_0$ is linear in c , and β and δ_1 depend linearly on Ω and also the Reynolds number parameter σ_r .

If we consider the Reynolds number as fixed, then as in Stewartson and Stuart we can set $|\sigma_r| = 1$ through the invariance

$$(\sigma_r, \Omega, c, \Phi, x) \rightarrow (L^2\sigma_r, L^2\Omega, Lc, L\Phi, s/L). \quad (2.5)$$

Thus given any single solution, a family of self-similar solutions exists as σ_r is varied, which become singular as $\sigma_r \rightarrow 0$. This does not exclude the existence of

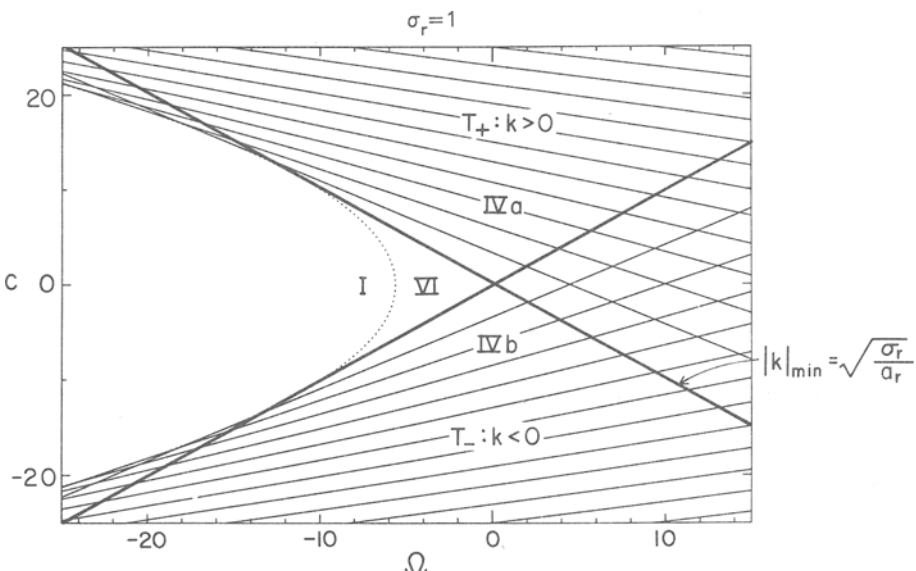


Figure 2. Lines of constant wavenumber for the plane wave solutions T_{\pm} for $\sigma_r > 0$.

families of solutions in a neighborhood of $\sigma_r = 0$, however, as is true in the instance of the plane wave solutions.

A plane-wave solution of wavenumber k , when cast in the framework of quasisteady solutions, will exist on the line

$$\Omega + kc = (a_i - d_0 a_r)k^2 + d_0 \sigma_r \quad (2.6)$$

in Ω - c parameter space. In this way these solutions are redundantly represented, although distinct solutions bifurcate from a given plane wave only for specific values of Ω and c . In Figure 2, lines of constant wavenumber (each corresponding to a single plane wave) are shown as a function of the two parameters for $\sigma_r > 0$. In this case we see there is a band of excluded k , and specifying Ω and c may result in describing zero (regions I and VI), one (regions IV) or both of the plane waves (elsewhere). For $\sigma_r < 0$ the regions IV disappear and all wave numbers are present, T_+ and T_- existing everywhere in parameter space except for the parabolic region I.

The second order complex ODEs (2.3) can be written as the first order system for $\Phi = u + iv$, which is of the form

$$\begin{aligned} u' &= p, \\ v' &= q, \\ p' &= -\delta_1 u + \beta v + (\delta_2 u - \gamma v)(u^2 + v^2) - c_1(p + a_0 q), \\ q' &= -\beta u - \delta_1 v + (\gamma u + \delta_2 v)(u^2 + v^2) + c_1(a_0 p - q). \end{aligned} \quad (2.7)$$

Due to the phase invariance of the GL equation

$$A \rightarrow Ae^{i\theta}, \quad (2.8)$$

this system possesses a rotational symmetry, given by

$$\begin{pmatrix} u \\ v \\ p \\ q \end{pmatrix} \rightarrow \begin{pmatrix} Q & 0 \\ 0 & Q \end{pmatrix} \begin{pmatrix} u \\ v \\ p \\ q \end{pmatrix}, \quad (2.9)$$

where Q is the rotation matrix

$$\begin{pmatrix} \cos \theta & -\sin \theta \\ \sin \theta & \cos \theta \end{pmatrix}$$

with θ arbitrary. This symmetry can be eliminated by writing Φ as an amplitude and phase, thus removing this apparent degree of freedom. Following Sirovich

and Newton [21], it is convenient to use the variables r , s , and w , where

$$\Phi = r^{1/2} \exp \left[i \int^X s dX \right], w = \frac{r'}{2r}, \quad (2.10)$$

in order to get a system of three first order ODEs. After some algebra we arrive at the reduced equations

$$r' = 2wr, \quad (2.11a)$$

$$s' = -\beta + \gamma r - 2sw - c_1(s - a_0 w), \quad (2.11b)$$

$$w' = -\delta_1 + \delta_2 r + s^2 - w^2 - c_1(a_0 s + w), \quad (2.11c)$$

which are a generalization of those of Newton and Sirovich, who sought simpler quasisteady solutions with $c = 0$ (and thus $c_1 = 0$).

Although this reduction to three dimensions makes much of the analysis of the complex Duffing equation considerably easier, a coordinate singularity is introduced at amplitude zero, and in general we must return to the 4-D system (2.7) for solutions where the amplitude vanishes at a point.

It is interesting to note that if we write

$$z = \frac{d}{dX} \log \Phi,$$

then

$$z = w + is$$

and Equations (2.11) may be written

$$\begin{aligned} r' &= 2r \Re \{ z \}, \\ z' &= -(\delta_1 + i\beta) + (\delta_2 + i\gamma)r - c_1(1 - ia_0)z - z^2, \end{aligned} \quad (2.12)$$

which we will find to be a useful representation.

2.3. Some general properties of the complex Duffing systems

We are primarily interested in classifying the spatial behavior of quasisteady solutions of the GL equation. In this section we consider some simple properties of the complex damped Duffing equation derived in the previous section and the related 4- and 3-D systems.

An important property of the quasisteady ODE systems concerns the divergence of the corresponding flows. For the 4-D system we find

$$\frac{\partial u'}{\partial u} + \frac{\partial v'}{\partial v} + \frac{\partial p'}{\partial p} + \frac{\partial q'}{\partial q} = -2c_1,$$

and similarly for a modified reduced system with coordinates (r^2, s, w)

$$\frac{\partial r^{2\prime}}{\partial r^2} + \frac{\partial s'}{\partial s} + \frac{\partial w'}{\partial w} = -2c_1.$$

Hence, as observed by other authors, when $c=0$ —in which case we seek solutions to the GL equation of the form

$$A = \Phi(x)e^{-i\Omega t}$$

—the phase spaces are volume preserving and thus no stable attractors can exist. We find that the introduction of the speed correction c acts as a damping on phase volumes and that in the case of positive c solutions may exist which approach an attractor in phase space as $X \rightarrow \infty$. Similarly, by the reflection symmetry, the phase spaces are volume expanding for $c < 0$, and attracting sets may exist as $X \rightarrow -\infty$. This phase space contraction does not imply that phase volumes remain bounded in a region of phase space, however, as occurs in the Lorenz equations for example, due to the existence of a Liapunov functional.

The discussion of stability of solutions in the phase space representations for Φ is relevant in determining the class of spatial variations possible for quasi-steady solutions of the GL equation. In particular, by monitoring the stability properties of a particular solution as a parameter is varied, one may determine bifurcations to new branches of solutions. Note however that these considerations are independent of the question of time dependent stability of quasisteady solutions.

In addition to the rotational symmetry (2.8), the GL equation possesses a reflection symmetry which is important in determining the structure of quasi-steady solutions. This $x \rightarrow -x$ symmetry of the GL equation manifests itself in the 4-D system (2.7) by the invariance

$$X \rightarrow -X, \quad c \rightarrow -c, \quad (u, v, p, q) \rightarrow (u, v, -p, -q), \quad (2.13)$$

and in the 3-D system (2.11) by

$$X \rightarrow -X, \quad c \rightarrow -c, \quad (r, s, w) \rightarrow (r, -s, -w). \quad (2.14)$$

Introduction of a nonzero wave speed c destroys the reflection symmetry of the steady equations which exists when $c=0$. It is easily shown that when $c \neq 0$ the equations cannot support symmetric solutions. However, when $c=0$ both symmetric and nonsymmetric solutions may exist.

When $c=0$, apart from solutions with the even reflection symmetry

$$\Phi(x) = \Phi(-x), \quad (2.15)$$

the equation can support odd solutions such that

$$\Phi(x) = -\Phi(-x), \quad (2.16)$$

where we have written the axis of symmetry at $x = 0$, although this is of course arbitrary. An important observation to make is that if a solution possesses the odd symmetry, it will be singular in the reduced 3-D phase space (2.11) because $\Phi(0) = 0$. It will therefore be necessary to study some quasisteady solutions (namely odd periodic and solitary waves) with the 4-D representation (2.7).

Solutions may possess both the odd and even symmetries about different origins, and we have found a fundamental branch of periodic solutions that bifurcates from the zero amplitude state with this double symmetry. This branch and its subsequent symmetry breaking bifurcations are summarized in Section 5.3. This double symmetry is the same as that of the cosine function, being even about 0 and $L/2$ and odd about $L/4$ and $3L/4$.

If we seek periodic solutions in the 3-D reduced representation, solutions of the complex Duffing equation may result which are periodic in two frequencies (quasiperiodic), and thus lie on a 2-torus in the 4-D phase space. For periodic solutions obeying the even symmetry (2.14) when $c = 0$ it follows that

$$\bar{s} \equiv \frac{1}{L} \int_0^L s(x) dx = 0, \quad (2.17)$$

and therefore the resulting solutions for Φ , the spatial part of the amplitude A , are also L -periodic when reconstructed by the transformation (2.10). Solutions of period L in the 3-D phase space do not have to obey this reflection symmetry, however, and we shall find such solutions numerically in Section 5. Also recall that this symmetry will always be violated for periodic solutions with $c \neq 0$. In these cases the spatial variation of the corresponding GL solutions will be quasiperiodic with two spatial frequencies, since $\bar{s} \neq 0$ in general, and thus the resulting spatial variation of A is

$$\Phi(X) = r^{1/2}(X) e^{ip(X)} e^{i\bar{s}X},$$

where $r(X)$ and $p(X)$ are of period L . The two spatial frequencies of A are thus $1/L$ and $\bar{s}/2\pi$, which in general will be incommensurate. Note however that the modulus of the amplitude remains periodic of period L .

3. Phase space structure of the 4-dimensional Duffing system

We consider the equations describing the spatial dependence of quasisteady solutions

$$\begin{aligned} u' &= p, \\ v' &= q, \\ p' &= -\delta_1 u + \beta v + (\delta_2 u - \gamma v)(u^2 + v^2) - c_1(p + a_0 q), \\ q' &= -\beta u - \delta_1 v + (\gamma u + \delta_2 v)(u^2 + v^2) + c_1(a_0 p - q), \end{aligned} \quad (3.1)$$

which were derived in Section 2 from the complex damped Duffing equation. The only fixed points of the system for (u, v, p, q) are the origin for all values of the coefficients (corresponding to the undisturbed state) and the ring of fixed points

$$u^2 + v^2 = \frac{\beta}{\gamma} \quad \text{when} \quad \Delta \equiv \delta_1 - \frac{\delta_2 \beta}{\gamma} \equiv \frac{d_r \Omega - d_i \sigma_r}{a_i d_r - a_r d_i} = 0$$

for all c . Recall that the existence of the rotational symmetry (2.9) implies that solutions in this phase space are only unique up to an arbitrary rotation. This ring of solutions occurs when the periodic plane wave orbits (2.1) of the GL equation coalesce to the spatially uniform state in a saddle-node bifurcation provided $\sigma_r < 0$. In the 4-D space the traveling waves are given by

$$u = \sqrt{r_T} \cos(s_T x + \theta), \quad v = \sqrt{r_T} \sin(s_T x + \theta), \quad (3.2)$$

where r_T and s_T are functions of the parameters as given in Equation (4.6) below, and θ is arbitrary.

The linearization about zero in the (u, v, p, q) phase space gives two eigenvalues satisfying

$$\lambda^2 + c_1(1 - ia_0)\lambda + \delta_1 + i\beta = 0 \quad (3.3)$$

with the other pair their complex conjugate. If we consider $\sigma_r \neq 0$ as fixed, then δ_1 and β cannot vanish as we vary Ω , and the origin will be a double spiral point in general. Therefore the only bifurcations that can occur from the origin will be of Hopf type, at which a pair of eigenvalues become pure imaginary and a branch of periodic solutions is possibly shed.

By setting $\lambda^2 = -\omega^2$ with ω real we find that

$$\omega^2 = (\beta/c_1)^2 = \delta_1 - a_0\beta \equiv \sigma_r/a_r,$$

so a Hopf bifurcation occurs on the lines

$$\beta = \pm \sqrt{\frac{\sigma_r}{a_r}} c_1,$$

or equivalently

$$\Omega = a_0 \sigma_r \pm \sqrt{\frac{\sigma_r}{a_r}} c \quad \text{provided } \sigma_r > 0 \text{ and } c \neq 0. \quad (3.4)$$

These two lines in parameter space correspond to the place where each of the plane waves (3.2) bifurcates from zero amplitude for supercritical Reynolds numbers.

With somewhat more algebra, one may consider the real parts of the eigenvalues in Equation (3.3) as a function of the two parameters. It is found that the

origin is a stable fixed point of the 4-D system in the region bounded by the lines (3.4) and $c > 0$. As σ_r approaches zero these lines coalesce, and for $\sigma_r < 0$ the origin is always a spiral saddle.

Normally the determination of the (spatial) stability of the periodic orbits bifurcating in a Hopf bifurcation would require a lengthy calculation. However, we know the branches of bifurcating plane wave solutions analytically and thus can infer their stability. Furthermore, by making use of the 3-D reduced representation for Φ in which these solutions are simply represented by fixed points, we are also able to determine secondary bifurcations from these plane waves. These results will be discussed in the next section.

In the special case $c = 0$ and $\sigma_r > 0$, a double Hopf resonance occurs at $\Omega = a_0\sigma_r$, when Ω is varied, due to the presence of symmetry. This type of bifurcation is a topic of current interest in the literature (e.g. [5]). From Equation (3.3), when $c = 0$ one complex conjugate pair of eigenvalues lies in the right half plane and the other in the left half plane. These eigenvalues coalesce on the imaginary axis when $\beta = 0$ ($\Omega = a_0\sigma_r$), noting that $\delta_1 > 0$ at the bifurcation. In this case we may expect periodic orbits (besides the plane waves), if not more complex dynamics, to exist nearby in parameter space.

Accordingly, we have found a third spatially periodic branch $P0$ of quasi-steady solutions bifurcating from the origin for fixed $c = 0$ and small $\beta > 0$ which displays the odd and even symmetries of Section 2.3. Also a family of quasiperiodic solutions (2-tori) bifurcates from the trivial state if we vary c away from zero for small β . These 2-tori lie on the same surface connecting the plane wave solutions and the symmetric branch $P0$ in the space of solutions. This situation has been analyzed using perturbation theory in [15] and is found in the numerical continuation of quasiperiodic orbits in Section 5.

4. Phase space structure of the 3-dimensional reduced ODE system

In this section we study the properties of the reduced system

$$r' = 2wr, \quad (4.1a)$$

$$s' = -\beta + \gamma r - 2sw - c_1(s - a_0w), \quad (4.1b)$$

$$w' = -\delta_1 + \delta_2 r + s^2 - w^2 - c_1(a_0s + w), \quad (4.1c)$$

which describes the spatial structure of quasisteady solutions of the GL equation whose amplitude is bounded away from zero. This 3-D phase space is geometrically far easier to work with than the 4-D space derived directly from the complex Duffing equation, and reveals several aspects of the dynamics of the Duffing equation more readily than the 4-D representation.

Recall that we consider $\gamma > 0$ and $\delta_2 < 0$ as fixed, β and δ_1 are proportional to the undetermined temporal frequency Ω , and c_1 is proportional to the undetermined speed correction c .

When $c_1 = 0$ the above system is the same as that studied by Sirovich and Newton [21] and in a slightly different form by C. Holmes and Wood [10] and

P. Holmes [12]. The first two authors concentrated on studying a single branch of periodic solutions. P. Holmes [12] studies small perturbations from the Hamiltonian case when $\beta = \gamma = 0$ (the nonlinear Schrödinger equation limit), and proves the existence of spatially periodic and quasiperiodic solutions. An analysis of the case $\delta_2 > 0$ has been carried out by Kopell and Howard [14] and arises in the analysis of reaction-diffusion equations.

We are primarily interested in transition from the laminar and plane wave states in Poiseuille flow. As each of these states is represented by a pair of fixed points in the reduced system, we seek solutions to the equations (4.1) which tend to these fixed points at spatial infinity. Thus we first need to discuss their existence and stability properties. In addition, with the introduction of the speed parameter c , we can look for attracting fixed points and more general attractors.

4.1. The invariant plane $r \equiv 0$ and the fixed points of laminar flow

An interesting aspect of the system (4.1) is that the plane $r \equiv 0$ is an invariant subspace. In this way the single fixed point of the 4-D system is transformed into a singular plane in the polar representation.

If we consider the reduced system in this subspace

$$s' = -\beta - 2sw - c_1(s - a_0w), \quad (4.2a)$$

$$w' = -\delta_1 + s^2 - w^2 - c_1(a_0s + w), \quad (4.2b)$$

then it is possible to find an analytic solution by creating the complex variable

$$z = w + is$$

as introduced in Section 2.2. The equations (4.2) reduce to

$$z' = -K_1 - K_2 z - z^2 \quad (4.3)$$

with solution

$$z = -\frac{1}{2}K_2 - \sqrt{\xi} \tan(\sqrt{\xi}X + i\rho), \quad (4.4)$$

where

$$K_1 = \delta_1 + i\beta, \quad K_2 = c_1(1 - ia_0), \quad \xi \equiv K_1 - \frac{1}{4}K_2^2 = \xi + i\eta,$$

and

$$\xi(\Omega, c) = \delta_1 - \frac{1}{4}c_1^2(1 - a_0^2), \quad \eta(\Omega, c) = \beta + \frac{1}{2}a_0c_1^2.$$

Here ρ is a real constant of integration, and the arbitrary shift in the origin of X is implicit.

There are two fixed points of the form $(0, s_0, w_0)$, which we call D_+ and D_- , corresponding to solutions of the quadratic (4.3) set equal to zero. It is interesting to note that this quadratic is identical to the eigenvalue equation (3.3) for the zero amplitude solution in four dimensions. Hence both values of w_0 must be negative if and only if the 4-D fixed point is stable. These fixed points have coordinates

$$D_{\pm} : \begin{cases} s_0 = \frac{a_0 c_1}{2} \mp \text{sgn}(\eta) \sqrt{\frac{|\xi| + \xi}{2}}, \\ w_0 = \frac{-c_1}{2} \pm \sqrt{\frac{|\xi| - \xi}{2}}. \end{cases}$$

Both fixed points exist for all values of the parameters, except when they coalesce at $\xi = \eta = 0$. A branch cut in parameter space has to be chosen in order to represent these fixed points continuously and unambiguously. We have chosen this cut to be $\eta = 0$ when $\xi \leq 0$, which corresponds to the parabolic segment

$$\Omega = a_0 \sigma_r - \frac{a_i c^2}{2|a|^2}, \quad \Omega \geq -a_0 \sigma_r.$$

On crossing this cut by varying Ω and c , D_+ and D_- swap identities.

The stability of these fixed points for the full 3-D system is determined from the eigenvalues

$$\lambda_1 = 2w_0, \quad \lambda_{2,3} = -(2w_0 + c_1) \pm i(2s_0 - a_0 c_1).$$

By considering the real part of the complex conjugate eigenvalues we find that D_+ is a stable point of the invariant plane and D_- is unstable, except on the branch cut, where both points are marginally stable, the complex conjugate eigenvalues having their eigenspaces lying entirely in the invariant plane.

In Figure 3 we illustrate the stability results for D_{\pm} in the 3-D phase space. As we can expect, the stability of the $\Phi = 0$ solution depends only on the real eigenvalue at D_+ and D_- , because λ_1 is proportional to the real part w_0 of z . Our results for the eigenvalue equation (3.3) therefore carry directly over, and we find that D_+ is stable in the region bounded by the lines (3.4) and $c > 0$ and D_- is unstable in the region bounded by these lines and $c < 0$, provided $\sigma_r > 0$. Elsewhere in parameter space these fixed points are saddles, as is always the case when $\sigma_r < 0$.

In general then, from (4.4), all orbits within the plane are bounded with the exception of at most two unbounded separatrices on which w is singular for finite X , which occurs when $\rho = 0$. The bounded orbits are heteroclinic between the spiral points D_- and D_+ . For parameter values on the branch cut, however, a change of stability occurs at these fixed points, and a vertical Hopf bifurcation takes place. All orbits in the plane are periodic except for a single separatrix on which $w \rightarrow \pm \infty$.

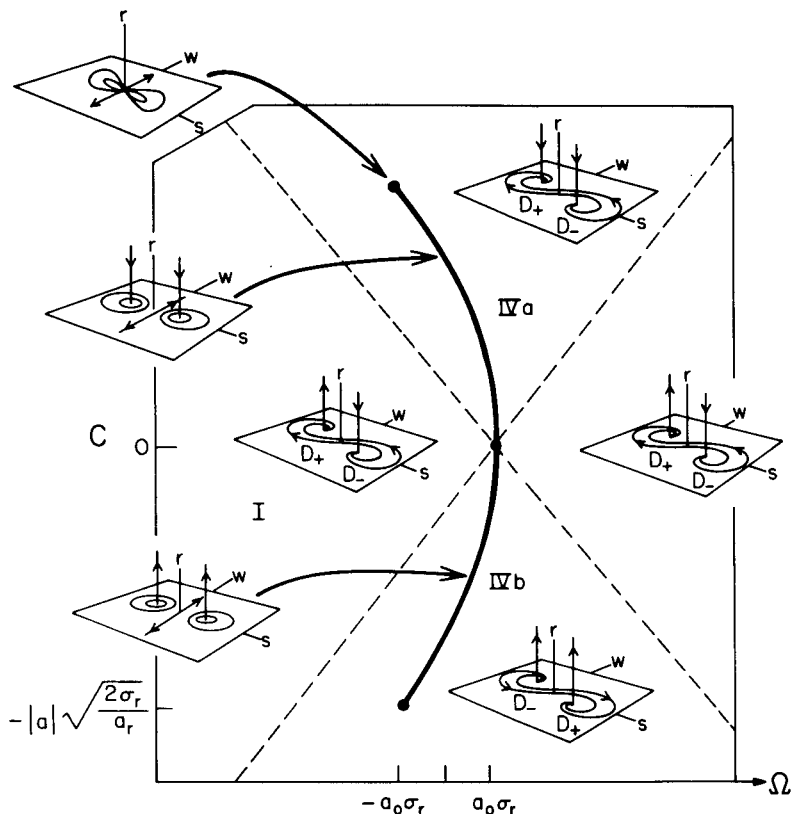


Figure 3. Phase portraits of the invariant plane for $\sigma_r > 0$. As $\sigma_r \rightarrow 0$ the regions IV disappear and only the phase portrait I persists for $\sigma_r < 0$. The heavy line denotes the branch cut.

One may ask what is the significance of a continuum of zero amplitude solutions represented by the orbits in the $r \equiv 0$ plane. Firstly, the fixed points D_{\pm} represent the exponential decay of solutions that tend to zero at plus and minus infinity, which is given by linearization of the GL equation for small amplitude. Thus solutions decaying to the laminar state at infinity must correspond to the orbits of the 1-D stable or unstable manifold of D_- or D_+ associated with the eigenvalue λ_1 .

The singularities for finite X represent solutions whose amplitude approaches zero, due to the algebraic singularity of Equation (4.4), which to leading order is of the form

$$w + \frac{c_1}{2} \sim \frac{1}{X - X_0}, \quad (4.5a)$$

$$s - \frac{a_0 c_1}{2} \sim -\frac{\beta}{3}(X - X_0)$$

as $X \rightarrow X_0$. This singularity in the invariant plane is accompanied in the third dimension by a decay of the amplitude to zero such that

$$r \sim r_1(X - X_0)^2 \quad \text{as } X \rightarrow X_0, \quad (4.5b)$$

where r_1 is undetermined. We note that this may still correspond to bounded motion for a solution of the GL equation, and that our choice of polar coordinates with $w = r'/2r$ fails to satisfactorily describe such solutions whose amplitude is zero at a point. In general this restricts our study in the reduced (r, s, w) space to solutions whose amplitude remains bounded away from zero.

The remainder of heteroclinic orbits in the invariant plane joining the fixed points D_- and D_+ are associated with the $\Phi \equiv 0$ solution and seem to be an artifact of the mathematical construction.

4.2. The fixed points of the plane wave solutions

The second pair of fixed points of the system (4.1) exists for $w = 0$ and correspond to the plane waves which were periodic solutions in the 4-D representation. These are given by

$$T_{\pm} : \begin{cases} r_T = \frac{\beta}{\gamma} + \frac{c_1^2 d_r}{2a_r \gamma^2} \pm \frac{c_1}{\gamma} \sqrt{\frac{c_1^2 d_r^2}{4a_r^2 \gamma^2} + \delta_1 - \frac{\delta_2 \beta}{\gamma}}, \\ s_T = \frac{c_1 d_r}{2a_r \gamma} \pm \sqrt{\frac{c_1^2 d_r^2}{4a_r^2 \gamma^2} + \delta_1 - \frac{\delta_2 \beta}{\gamma}}, \\ w_T = 0. \end{cases} \quad (4.6)$$

Hence the corresponding GL solutions become

$$A = r_T^{1/2} e^{is_T x} e^{-i(\Omega + s_T c)t},$$

recalling that a wave of given wavenumber $k = s_T$ lies on a line in parameter space given by Equation (2.6).

In order for T_+ or T_- to exist we require that these fixed points be real and that $r_T > 0$. When $c = 0$ these points are images of each other under the reflection symmetry and exist provided both

$$\Delta \equiv \delta_1 - \frac{\delta_2 \beta}{\gamma} \quad \text{and} \quad \frac{\beta}{\gamma}$$

are nonnegative. If $c = 0$, a necessary condition for the existence of periodic orbits is the existence of the fixed points T_{\pm} [15].

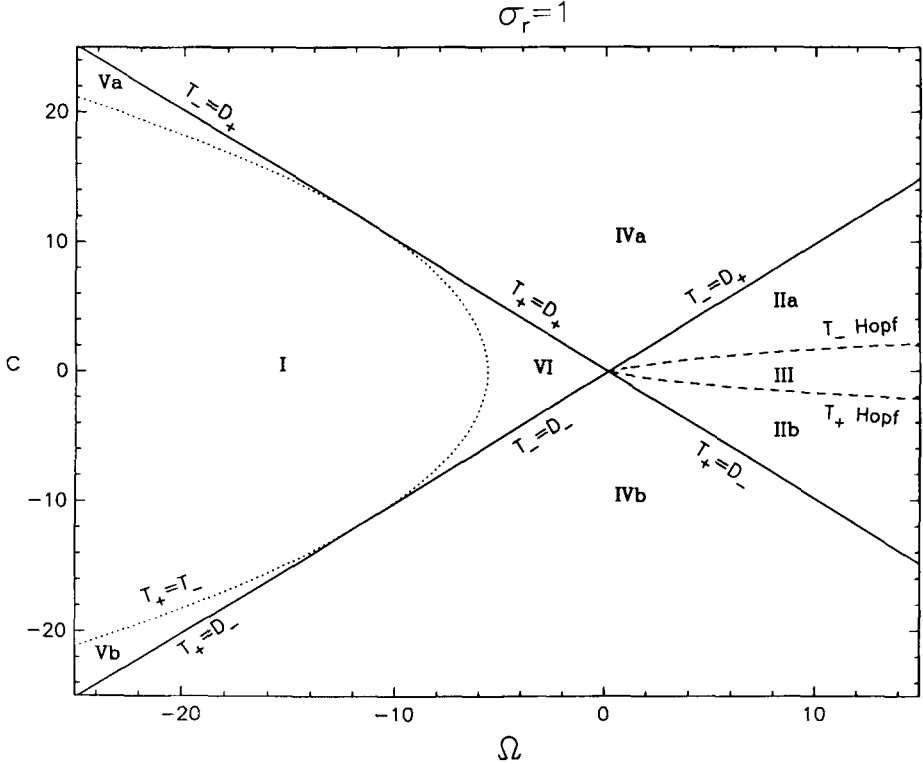
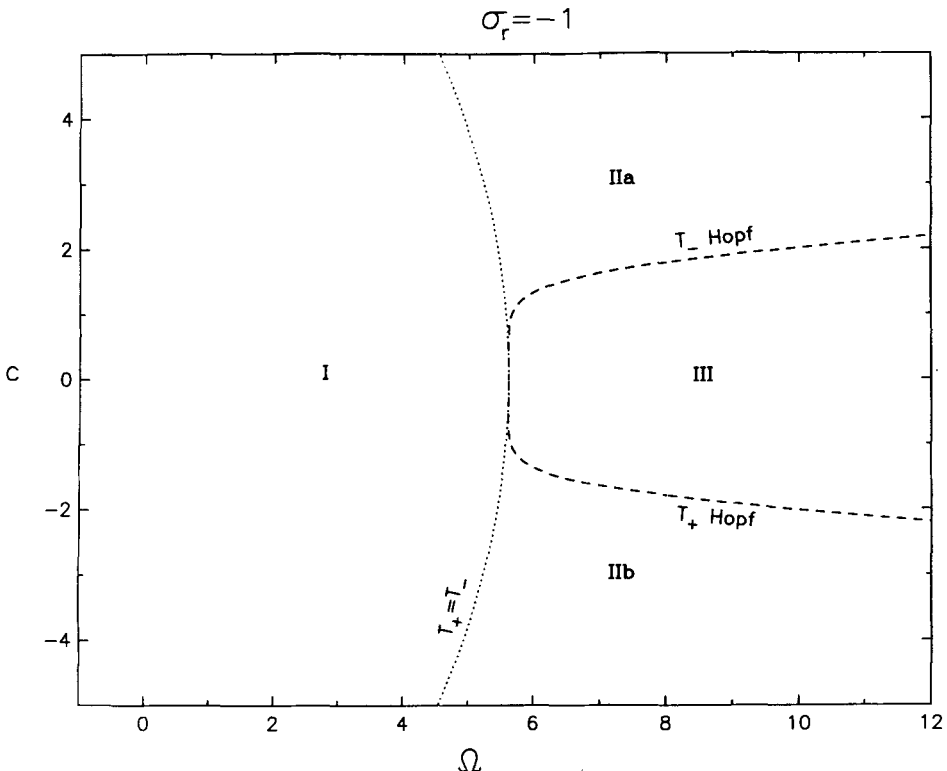


Figure 4. Stability diagram for the four fixed points of the reduced system, $\sigma_r = 1$.

The characteristic equation of the linearization about these plane wave fixed points is given by

$$\lambda^3 + 2c_1\lambda^2 + [c_1^2 + (2s_T - a_0 c_1)^2 - 2\delta_2 r_T] \lambda - 2r_T [c_1 \delta_2 + \gamma(2s_T - a_0 c_1)] = 0. \quad (4.7)$$

In studying the stability of the plane wave fixed points we shall refer to regions of parameter space shown for the Poiseuille coefficients in Figures 4 and 5 and Table 1. Figure 4 illustrates the regions relevant in studying the existence and stability of both pairs of fixed points as a function of the two parameters for $\sigma_r = 1$, and similarly for Figure 5 when $\sigma_r = -1$. Recall that we can always scale nonzero $|\sigma_r|$ to 1 by the invariance (2.5), so these diagrams are representative of super- and subcritical Reynolds numbers respectively. Table 1 indicates the number of positive and negative eigenvalues associated with each of the four critical points T_{\pm} and D_{\pm} in the different regions of parameter space. This table and figures were constructed by solving (4.7) numerically for the Poiseuille parameters as well as by considering bifurcations from the fixed points as described below. In general we find one pair of the eigenvalues of T_{\pm} is complex

Figure 5. Stability diagram, $\sigma_r = -1$.

conjugate, although in segments of region IV when $\sigma_r > 0$ and region II when $\sigma_r < 0$ all the eigenvalues can be real; this has no bearing on the stability properties which we discuss here.

In order to determine bifurcations from the plane wave fixed points we examine when an eigenvalue is zero or when there is a pure imaginary pair of eigenvalues. There are two cases for a zero eigenvalue. The first occurs when a traveling wave bifurcates from zero amplitude so that $r_T = 0$. At this point one of the T fixed points coalesces with a D fixed point which occurs on the lines (3.4). In this way the Hopf bifurcation describing this phenomenon in the 4-D system has been reduced to a regular bifurcation of steady solutions in the reduced system. The second case of a zero eigenvalue occurs when the square root in (4.6) vanishes and T_+ and T_- coalesce in a so-called saddle-node bifurcation, although this is really a limit point and no new branches are created there. The locus of this limit point gives the region for the existence of T_{\pm} and is given by

$$\Omega \geq d_0 \sigma_r - \frac{d_r c^2}{4\gamma |a|^2},$$

Table 1
Numbers of Stable and Unstable Eigenvalues of the Critical Points
in the Regions of Ω - c Parameter Space^a

Region	Critical point stability.			
	Number of (negative, positive) eigenvalues.			
	T_+	T_-	D_+	D_-
I	—	—	(2, 1)	(1, 2)
IIa	(2, 1)	(3, 0)	(2, 1)	(1, 2)
IIb	(0, 3)	(1, 2)	(2, 1)	(1, 2)
III	(2, 1)	(1, 2)	(2, 1)	(1, 2)
IVa	(2, 1)	$r_T < 0$	(3, 0)	(1, 2)
IVb	$r_T < 0$	(1, 2)	(2, 1)	(0, 3)
Va	(2, 1)	(3, 0)	(2, 1)	(1, 2)
Vb	(0, 3)	(1, 2)	(2, 1)	(1, 2)
VI	$r_T < 0$	$r_T < 0$	(2, 1)	(1, 2)

^aThe regions in the bottom half of the table exist for $\sigma_r > 0$ only.

which corresponds to excluding region I. Ensuring that $r_T > 0$ also excludes region VI, and we find only one plane wave solution exists in the regions IV when $\sigma_r > 0$.

In we seek Hopf bifurcations by setting $\lambda^2 = -\omega^2$ with ω real in (4.7), a cubic equation in c_1^2 results after eliminating ω , s_T , and r_T . We have solved this equation numerically and find a locus of Hopf bifurcations from T_+ and T_- occurs in Ω - c space for σ_r either side of critical. From the Hopf bifurcation theorem, given that we are not in a degenerate situation, branches of periodic orbits must exist in a neighborhood of these fixed points. These have been found numerically as described in Section 5. It is interesting that returning to the original representation for Φ , this locus of secondary bifurcations is to spatially quasiperiodic solutions, which are 2-tori in the 4-D phase space. This follows from the discussion in Section 3.4, as $c \neq 0$ for these solutions. This bifurcation to a 2-torus was also found by C. Holmes [11] using center manifold theory on the GL equation. By comparing Figures 2 and 4 we observe that each plane wave of a given wavenumber undergoes such a secondary bifurcation. The situation is also true when $\sigma_r < 0$, where a given plane wave may undergo one or three bifurcations.

We now summarize the most important features of our stability results when $c > 0$. We find that T_- is an attracting fixed point in regions IIa and Va of parameter space, as is the zero amplitude fixed point D_+ in region IVa. Region IV exists only for $\sigma_r > 0$, and diminishes in size as $\sigma_r \rightarrow 0$, when regions II and V coalesce. Otherwise all the critical points are saddles. Regions IV, V and VI are the only sectors of parameter space which are unique to $\sigma_r > 0$. When $c < 0$, from the invariance (2.14), the results are analogous by reversing stabilities and swapping the subscripts + and - of the critical points.

5. Spatially periodic and quasiperiodic solutions

In this section we summarize some of our numerical results concerning periodic solutions of the 4-D and 3-D Duffing systems. We concentrate primarily on those aspects which are relevant to our later discussion of solitary-wave-type solutions of the GL equation. For a more thorough description see [15], where in addition perturbation expansions are developed for some of these solutions.

5.1. Periodic orbits of the reduced system: $\sigma_r < 0$

In the study of the 3-D system (4.1) with $c = 0$, both Sirovich and Newton [21] and Holmes and Wood [10] discuss a branch of periodic orbits that exists for a range of the parameters in the phase space (r, s, w) and bifurcates from the spatially uniform solution, which occurs when the pair of plane wave solutions (2.1) coalesce in the limit of vanishing wavenumber. If the $|\delta_i|$ are scaled to unity, they consider having $\delta_1 = \delta_2 = -1$, in which case the uniform solution $(r, s, w) = (\beta/\gamma, 0, 0)$ exists only when $\beta/\gamma = 1$. As they consider that $\sigma_r > 0$ in the GL equation, this implies that $d_r < 0$ for this bifurcation to occur. Holmes and Wood continued the branch and deduced that it is most likely created in a heteroclinic bifurcation from the analytically known solitary wave solution which we describe in Section 6.2. This solution is of the form of a breather, in that it decays to zero at plus and minus infinity, connecting D_+ and D_- in the reduced phase space.

We note that the bifurcation from the uniform solution also occurs for the Poiseuille case $d_r > 0$ if we consider $\sigma_r < 0$. The exact solitary wave solution does not exist for any value of Ω for subcritical σ_r , and thus we continued the branch numerically away from the bifurcation point ($\Omega = -d_0$ for $\sigma_r = -1$) to see where it leads. Starting from an initial guess found by analytically perturbing $r = \beta/\gamma$ for small β , we continued the branch using the program AUTO developed by Doedel and Kernevez [3]. This software is able to perform accurate continuation and bifurcation analysis for solution branches of systems of ODEs by a collocation method on an adaptive mesh. In particular the program is able to follow periodic orbits and generate the Floquet multipliers. For the reduced system one multiplier σ_0 is always at 1 due to the translation invariance on a periodic orbit. The other multipliers $\sigma_{1,2}$ satisfy

$$\sigma_1\sigma_2 = \exp(-2c_1L), \quad (5.1)$$

where L is the period.

The Floquet multipliers indicate a normal pitchfork bifurcation (including symmetry breaking) when an exponent passes through 1, a period doubling bifurcation when it crosses -1 , and—if the exponents cross the unit circle as a parameter is varied—the possibility of bifurcations to orbits of higher multiples of the period L and invariant 2-tori (two frequency motion) and perhaps spatial chaos. When both multipliers lie inside the unit circle, the orbit is stable. In the case $c = 0$, the two nontrivial multipliers can be either real and reciprocals of each other or complex conjugate and on the unit circle.

Figure 6 is a diagram of two of the branches $S1$ and $S2$ of periodic solutions that we have found when $\sigma_r = -1$. Branch $S1$ is the primary branch which

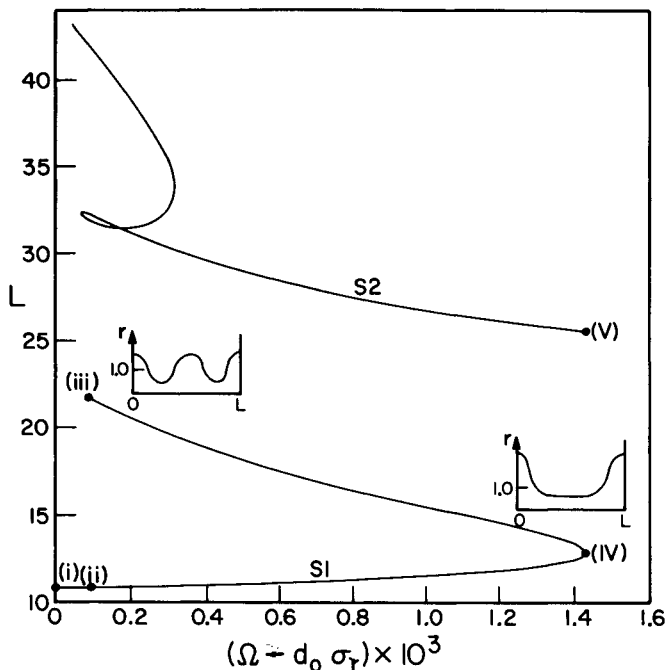


Figure 6. Bifurcation diagram for the period of two branches of symmetric periodic orbits, $\sigma_r = -1$. Point (i) is the uniform solution where $T_- = T_+$.

bifurcates from the uniform solution at $\beta = \gamma$ ($\Omega = d_0$). The modulus of the amplitude of the solutions on these branches remains essentially near unity and slowly varying, and they have the even symmetry. The resulting solutions suggest the existence of symmetric periodic envelope solutions in plane Poiseuille flow at Reynolds numbers less than Re_c that only slightly modify the form of the Tollmien-Schlichting wave. We have found others of higher period; however, all of these lie in a small neighborhood of the critical value of Ω , as do the ones of lower period shown.

By monitoring the Floquet multipliers and plotting out the solutions along the branches, we find that $S2$ is born in period doubling bifurcations from $S1$. We have marked points where such bifurcations occur in Figure 6. Point (i) is the primary bifurcation from the uniform solution. Period doublings occur from (ii) to (iii) and (iv) to (v). In fact we suspect there is at least one period doubling cascade occurring which may lead to the existence of chaotic orbits close to the uniform state at $\beta = \gamma$. This behavior is in accordance with the more detailed local analysis performed by Holmes and Wood [10], whose normal form analysis and numerical work suggests the local existence of quasiperiodic and perhaps chaotic orbits.

In any case we find that for the Poiseuille coefficients the bounded solutions found for $c = 0$ exist only in a small neighborhood of the bifurcation point. Also, unlike the cases discussed by other authors, for the Poiseuille parameters the

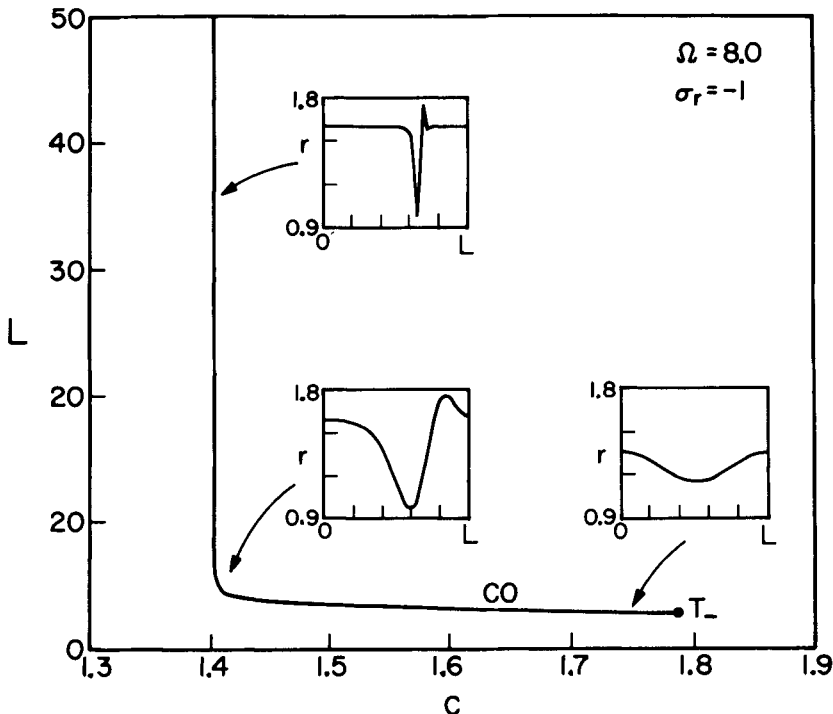


Figure 7. Branch C_0 of periodic orbits of the reduced system in region III, for fixed $\Omega = 8.0$ and $\sigma_r = -1$. The branch bifurcates from the fixed point T_- , and approaches a homoclinic orbit as c is decreased.

uniform state is subcritical and temporally unstable, as is the bifurcating periodic branch.

We can continue solutions in the parameter c , and thus search for (spatially) stable periodic orbits which correspond to 2-tori of the GL equation in space and time. We show an example of a computation when we decreased c for $\Omega = 8.0$ from the Hopf bifurcation point of the fixed point T_- , and the resulting branch C_0 is shown in Figure 7. We find that the bifurcation is supercritical, and the stable periodic orbit that is shed has a continuation to orbits of period tending to infinity. The branch is stable up to at least period 8, when we can no longer accurately compute the Floquet multipliers. We have been able to compute orbits of period greater than 10^6 , providing good evidence that the branch converges to a homoclinic orbit of the plane wave fixed point. In this way it appears that there is a curve in Ω - c parameter space at which this homoclinic orbit exists (see Section 6 for a discussion of homoclinic and heteroclinic orbits).

5.2. Periodic orbits of the reduced system: $\sigma_r > 0$

We start with a discussion of the periodic solutions in the 3-D phase space for $c = 0$, and can set $\sigma_r = 1$ for the general supercritical case. We found symmetric

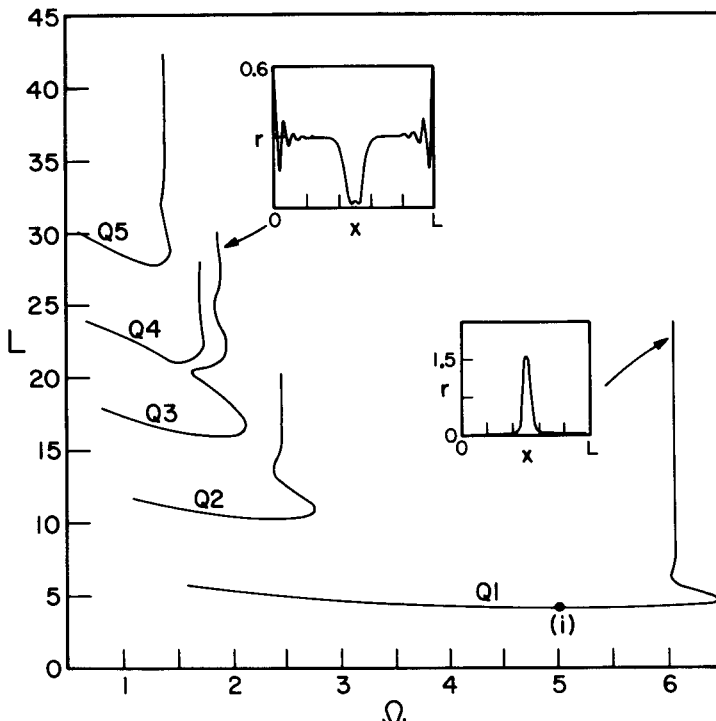


Figure 8. Period versus Ω for the symmetric Q branches of the reduced system, $c = 0$ and $\sigma_r = 1$.

periodic orbits initially using a shooting method. Once a solution was converged to at a particular value of Ω , we could then continue it using the code AUTO. We have been able to find five symmetric branches with this procedure, the number limited by our primitive starting procedure.

Figures 8 and 9 display a set of solution branches for the system (4.1) with vertical axis the period and L^2 norm for (r, s, w) respectively, and horizontal axis Ω . All possess the reflection symmetry (2.14). These solutions represent families of spatially symmetric periodic envelopes of Tollmien-Schlichting waves and travel downstream at the group velocity for $\text{Re} > \text{Re}_c$.

The left hand end of each branch shown corresponds to the formation of a singularity in the periodic orbit. In each case the amplitude of w tends to infinity and r and s tend to zero simultaneously. We find that the solution tends to have the asymptotic form (4.5), which indicates the amplitude of the solution is passing through zero as Ω is varied. This reflects the shortcoming of the polar representation of the amplitude that we use. In order to continue these branches it is necessary to use the full 4-D system (2.7) for the amplitude, and in fact we shall find that they all bifurcate from a periodic orbit with odd symmetry where $\Phi(0) = \Phi(L/2) = 0$.

At the right hand end of each branch in Figure 8 the period is becoming large, and in each case the numerical evidence suggests that the branch is being created

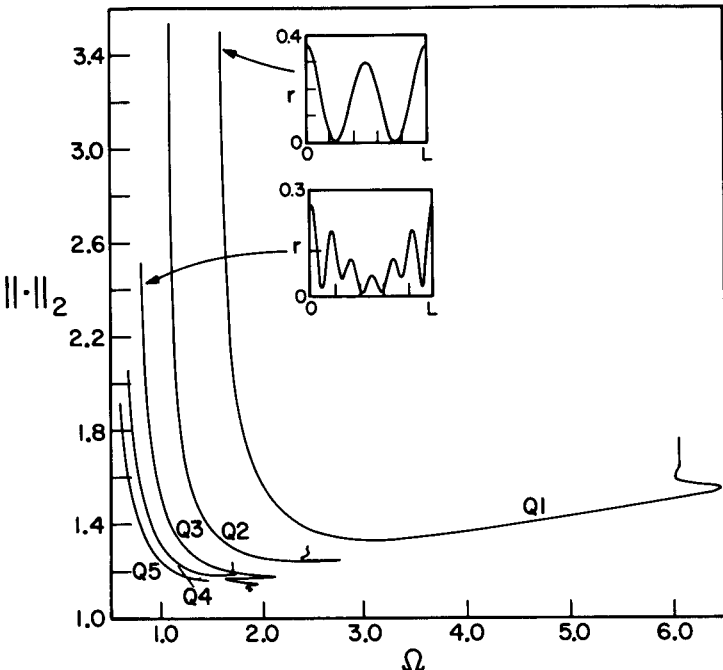


Figure 9. L^2 norm versus Ω for the Q branches, $c = 0$ and $\sigma_r = 1$.

in a heteroclinic bifurcation. Our conclusions are drawn from the examination of the periodic orbits of large period, and the further numerical work of Section 6.3.

Firstly, the evidence is strong that the branch $Q1$ is created in the bifurcation of the breather solitary wave known analytically (see Section 6.2). In particular the value at which this exact solution exists is $\Omega = 6.058$, in agreement with our continuation to very high period using the program AUTO. Similarly, the branches $Q2$, $Q4$, and $Q5$ consist of solutions for which the amplitude approaches zero for an increasingly large proportion of their period. In this way it appears that these periodic orbits are also approaching a pair of heteroclinic connections between D_+ and D_- , one lying in the $r \equiv 0$ plane and the other lying above it. Such solutions become solitary envelopes of the Tollmien-Schlichting waves for plane Poiseuille flow and travel at the group velocity. We recompute these and more solutions connecting D_+ to D_- in Section 6.3.

The fate of branch $Q3$ is quite distinct from the others, however. It comes very close to the plane wave fixed points T_+ and T_- and has amplitude modulus always staying bounded above zero, which strongly suggests at this value of $\Omega \approx 1.85$ a heteroclinic loop exists between the plane wave fixed points.

We now briefly discuss continuation of periodic orbits by varying c . Starting at the orbit on the symmetric branch $Q1$ at $\Omega = 5.0$ [point (i)], we fixed Ω and continued in c for the equations (4.1). Figure 10 shows the branch $C1$ that results. We find that for this value of Ω there are four more periodic orbits with $c = 0$, at points labeled (ii) and (iii). These solutions are nonsymmetric, and the mean of s

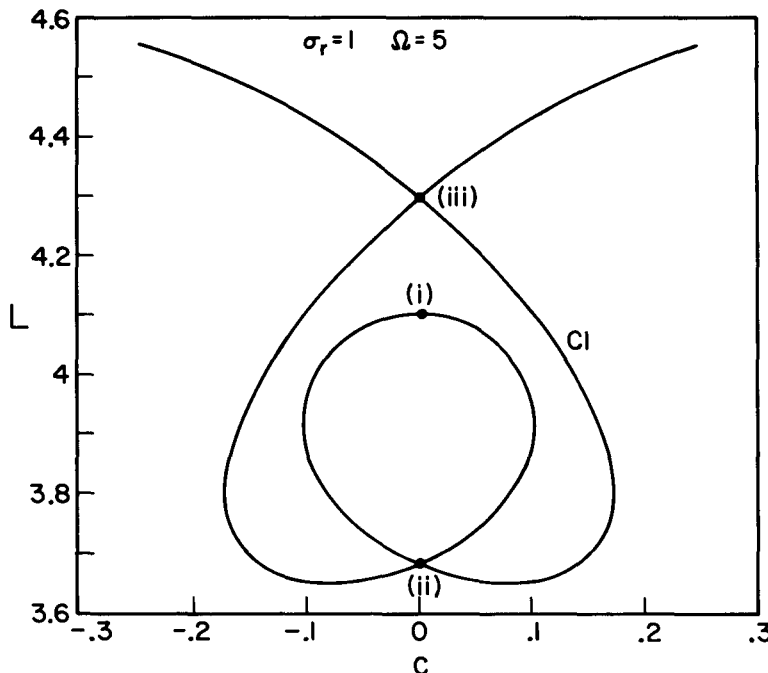


Figure 10. Continuation of point (i) on branch $Q1$ in c for fixed $\Omega = 5.0$. The resulting branch $C1$ of nonsymmetric periodic orbits is also not linearly stable.

over one period is nonzero, indicating the corresponding GL solution is quasi-periodic as discussed in Section 2.3. Thus the branch $C1$ lies on a surface of 2-torus solutions in the product space of quasisteady solutions and the 2-D parameter space.

At each of the points (ii) and (iii) there is a pair of solutions which are reflections of each other. We have continued these solutions in Ω with fixed $c = 0$ and show one of the resulting nonsymmetric branches $N1$ in Figure 11. Note that a twin branch to the one shown must also exist under the reflection symmetry. We find that along this branch \bar{s} is nonzero as defined in equation (2.17), so that the solutions on this branch, although periodic in the reduced phase space, are quasiperiodic with two frequencies when the spatial form of the corresponding GL solution is obtained.

We find that the solutions at the right hand end of $N1$ are becoming singular, which suggests that this branch, like the symmetric Q branches, is bifurcating from a branch with odd symmetry at $\Omega \approx 10.4$. It is also interesting that the left hand end of $N1$ increases to very large period, and on inspecting such solutions as in the insets of Figure 11, we find that this branch seems to bifurcate in a homoclinic bifurcation from the plane wave T_- , as does its reflection from T_+ . In this way we have strong evidence that homoclinic orbits to the plane wave fixed points exist for $c = 0$ at a value of $\Omega \approx 5.49$.

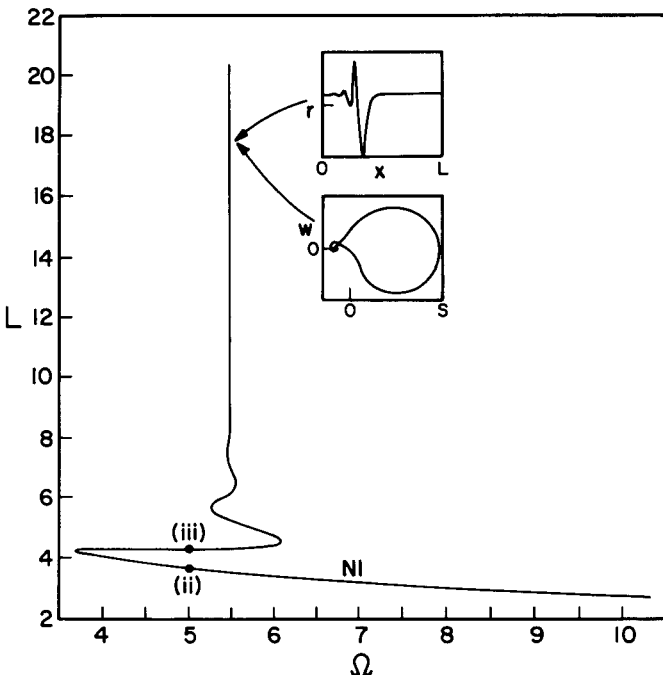


Figure 11. Branch $N1$ of nonsymmetric periodic solutions of the reduced system, $c = 0$.

Now we consider the continuation of periodic orbits bifurcating from the plane wave fixed point T_- at the boundary of the regions II and III in parameter space for $\sigma_r = 1$ and fixed Ω . In Figure 12 we show the maximum modulus squared (maximum of r) versus c for the $C2$ branch at $\Omega = 5.0$. The branch undergoes at least two supercritical period doubling bifurcations, the first one to branch $C3$. The behavior differs from the case $\sigma_r = -1$ in Figure 7 in that the primary branch extends to $c = 0$, where it becomes singular though the period and amplitude remain bounded, due to bifurcation from a periodic solution $P0$ with odd symmetry as for the Q branches. In this way such a branch and its twin for $c < 0$ connect the plane wave solutions with a family of 2-tori through the periodic orbit $P0$ at $c = 0$.

5.3. Periodic orbits in the 4-D phase space for $\sigma_r > 0$

From the results of the last section we are led to search for a branch of quasisteady spatially periodic solutions of the GL equation with odd symmetry for $c = 0$ and $\sigma_r = 1$. Such a branch is singular in the reduced system due to the amplitude vanishing at a point, thus forcing us to consider the 4-D complex Duffing system.

Using perturbation theory, we have been able to find a small amplitude expansion for a periodic orbit bifurcating from $\beta = 0$ ($\Omega = a_0\sigma_r$), which has both odd and even symmetries [15]. C. Holmes [11] was able to prove the existence of

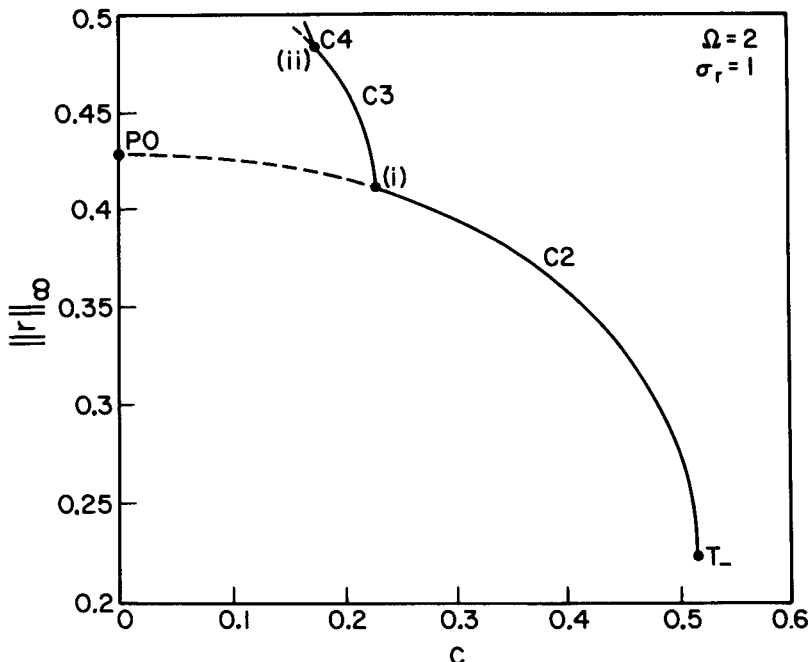


Figure 12. Continuation in c of Hopf bifurcating branch from T_- into region III. Solid lines are stable periodic orbits. Supercritical period doubling bifurcations occur at (i) and (ii).

this third branch bifurcating from the trivial state (in addition to the pair of plane waves). With this as a starting point, we continued to finite amplitude numerically. Because the rotational symmetry in the 4-D system leads to a singular Jacobian, a standard continuation procedure for periodic solutions fails. By adding the artificial perturbation parameter ϵ in the periodic boundary condition on u , where

$$u(0) = u(L)(1 - \epsilon),$$

we could continue the branch satisfactorily as a boundary value problem using the code **AUTO**. In addition to the above boundary condition and periodicity for v , p , and q , we imposed two integral constraints to fix the translation and phase invariances, and continued in the three free parameters Ω , the period L , and ϵ . During the continuation we insisted that $\epsilon < 10^{-8}$, so that an accurate solution to the actual periodic problem was ensured. We were also able to monitor the Jacobian of the extended system to find bifurcations.

Apart from the primary branch which we call P_0 , we have found a new branch P_1 bifurcating from it in a spontaneous symmetry breaking. P_1 has odd symmetry, so it is still singular in a 3-D representation, but no longer preserves the reflection symmetry. We were also able to recompute the symmetric Q branches using the 4-D code. In Figures 13 and 14 we show the bifurcation

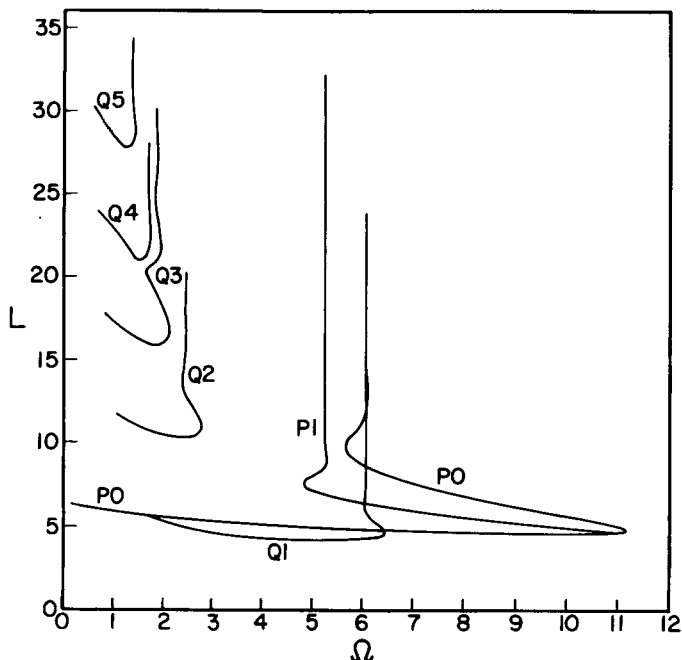


Figure 13. Bifurcation diagram for the period of solutions in the 4-dimensional complex Duffing phase space, $c = 0$.

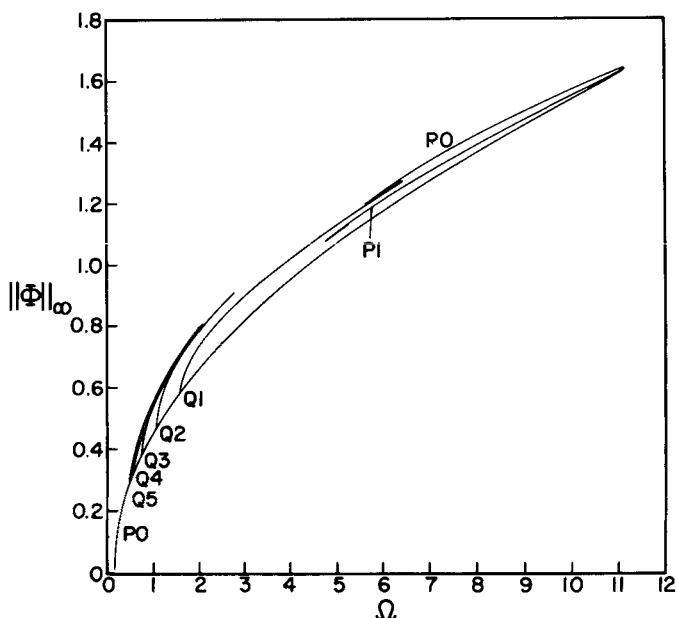


Figure 14. Bifurcation diagram for the maximum modulus of solutions in the 4-dimensional complex Duffing phase space, $c = 0$.

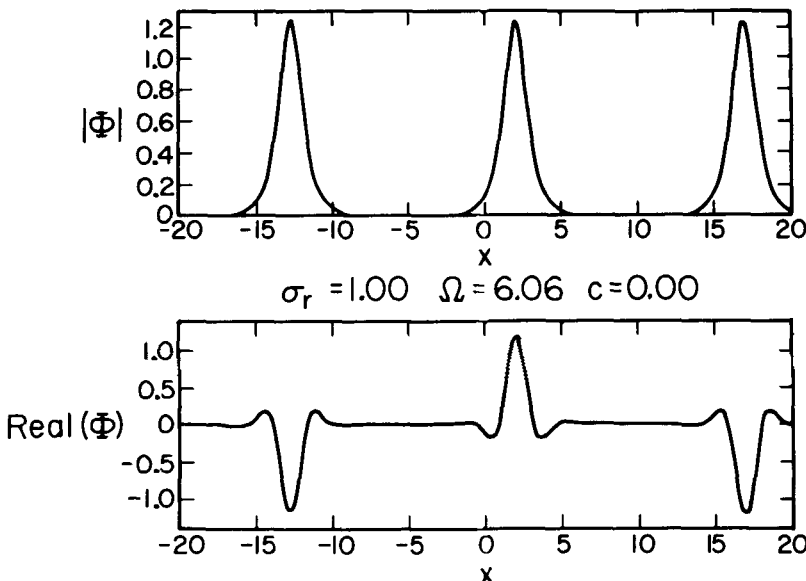


Figure 15. $1\frac{1}{2}$ periods of an orbit of high period on branch P_0 , approaching a pair of Q_1 breather solitary waves.

diagrams for all these solutions as a function of period L and maximum modulus $\|\Phi\|_\infty$ of the amplitude respectively. The latter is a convenient choice, as one can also plot quasiperiodic solutions on such a bifurcation diagram, whose period is strictly infinite.

We can now directly observe that the Q branches all bifurcate from P_0 with the loss of odd symmetry. Although we have been unable to compute Floquet multipliers in the 4-D continuation, there are only two nontrivial multipliers which satisfy Equation (5.1) and thus $\sigma_1\sigma_2=1$ when $c=0$. We expect that the multipliers will be at $+1$ when Q_1 bifurcates and at -1 when Q_2 bifurcates in a period doubling, and that they will move around the unit circle back to $+1$ for decreasing $\Omega > a_0\sigma_r$. We thus conjecture that an infinite number of branches bifurcate from P_0 of period nL/m when the multipliers lie at $e^{\pm 2\pi im/n}$.

We have already commented on the large period limits of the Q -branches. We see that for large period branches Q_1 and P_0 appear to coalesce. This is a particularly interesting bifurcation, as P_0 possesses odd and even symmetries whereas Q_1 is even only. We conclude that there is a “period doubling at infinity,” where Q_1 is a single hump tending to a breather solitary wave [in fact an exact solution shown in Figure 19(a)] and P_0 is a two hump solution approximating two Q_1 humps of opposite phase. See Figure 15. The large period limit of the branch P_1 also yields a breather solution, but with odd symmetry only, as shown in Figure 16.

We cannot continue periodic solutions to nonzero c in the 4-D space, as they become quasiperiodic; however, as with the case of the Q branches, we can interpolate between the results of the 3- and 4-D complex Duffing representa-

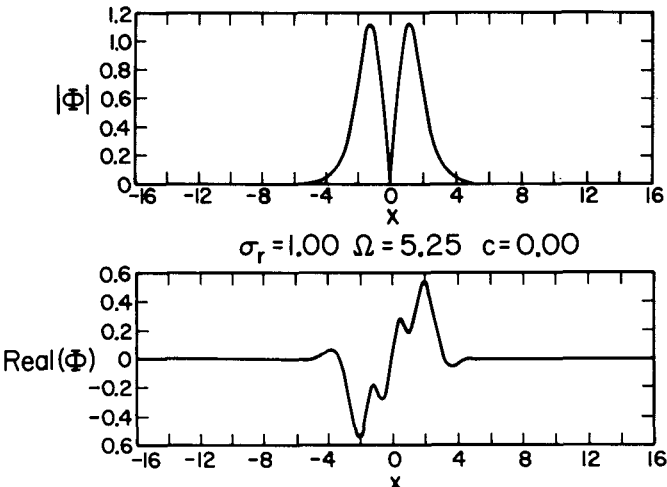


Figure 16. A single period of a solution of large period on branch $P1$, approaching a breather solitary wave of odd symmetry.

tions which complement each other. We are able to conclude that the continuation of $P0$ in c is the surface of 2-torus solutions mentioned earlier which bifurcates from T_+ and T_- in a Hopf bifurcation.

In conclusion to this section, we have been able to find a complicated structure of periodic solutions for the systems (2.7) and (4.1) using the parameter values (2.4) appropriate to Poiseuille flow. The solutions of the GL equation that result are thus periodic or quasiperiodic in space and simply periodic in time, provided one is moving in a frame of reference of speed c . For $c = 0$ we appear to have found a large class of solitary wave solutions for $\sigma_r > 0$. For $c > 0$ we have also found (spatially) stable quasiperiodic solutions for σ_r either side of critical.

The complexity of the structure of periodic solutions is somewhat typical in that complicated dynamics (in this case spatial) may occur in continuous systems with simple nonlinearities in only three dimensions. The symmetries in the GL equation also play an important role in determining the structure of the periodic solutions. We stress that due to the complexity of this structure, our classification of periodic orbits is far from complete. One reason we have not pursued this further is that due to the discovered nonuniqueness and lack of any selection criterion for the free parameters Ω and c , it is unclear which of the branches of periodic orbits, if any, are physically relevant.

6. Solitary wave solutions and transitions from the laminar and plane wave states

In this section we consider quasisteady solutions of the GL equation which are asymptotic at plus or minus infinity to either the trivial laminar state or plane wave states. Hence we study orbits in the 3-D reduced phase space which are the stable or unstable manifolds of the critical points D_{\pm} and T_{\pm} . In particular we are interested in homoclinic and heteroclinic orbits connecting these critical

points which result in solitary wave solutions. Recall that T_{\pm} and D_{\pm} have physical significance in the Poiseuille problem and that connections between these points in phase space may indicate similar connections between traveling waves and the laminar state in the fluid equations from which the GL equation is derived. In addition we numerically find solutions that are asymptotic from the laminar state and plane waves to some of the attracting quasiperiodic solutions described in the previous section and also to apparently spatially chaotic states. In so doing we are able to find a large class of quasisteady solutions describing a transition from the laminar state to a finite amplitude disturbance.

6.1. Classification of solitary wave connections in phase space

We now discuss the possible heteroclinic and homoclinic connections that could exist for the system of three ODEs under consideration as the parameters Ω and c are varied. Some of these solutions have been found previously in analytic form by other authors, and our numerical work of Section 6.3 gives strong evidence for the existence of many others.

In the light of the stability calculations for the critical points D_{\pm} and T_{\pm} , we can expect solitary wave solutions to exist for either a continuum or discrete values of Ω and c by considering the dimensionality of the fixed points' stable and unstable manifolds.

Homoclinic orbits can exist only at the fixed points T_{\pm} , which we label

$$H0: T_+ \rightarrow T_+ \text{ and } T_- \rightarrow T_-.$$

However there are four main types of heteroclinic orbits joining distinct fixed points, illustrated in Figures 17 and 18. First we know a continuum of connections exists of the type

$$H1: D_- \rightarrow D_+$$

in the $r \equiv 0$ plane for almost all values of the two parameters Ω and c , although these represent the trivial $A \equiv 0$ solution.

A connection of the type

$$H2: D_+ \rightarrow D_-$$

for which the modulus of the amplitude is positive was shown to exist by Hocking and Stewartson [8] for a discrete value of Ω and $c = 0$; they simply wrote down this breather type solitary wave solution in closed form, which we will discuss below. Note that a heteroclinic orbit of type $H2$ corresponds to a homoclinic orbit of $(0, 0, 0, 0)$ for the 4-D system (2.7). Any connection to or from the laminar state in the reduced representation must consist of the 1-dimensional stable or unstable manifolds of D_- and D_+ respectively. When $c = 0$ the connection of type $H2$ must be symmetric, and such a solution would in general not be expected for a continuum of Ω . We have numerical findings that strongly suggest that many more if not an infinite number of symmetric breather solutions

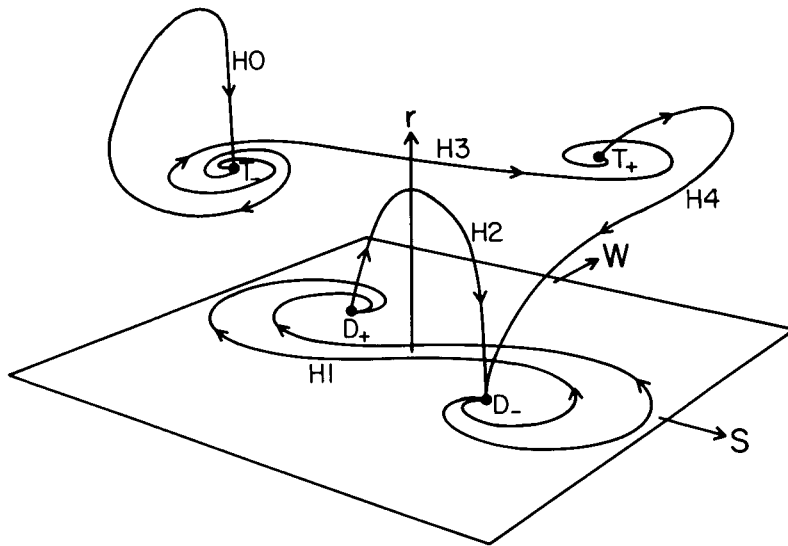


Figure 17. Orbits in the reduced phase space as examples of homoclinic (H_0) and heteroclinic connections (H_1-H_4).

exist for a discrete spectrum of Ω , which we discuss in Section 6.3. When $c \neq 0$ one would expect breather solutions to exist for discrete values of the two parameters only (i.e. a codimension-2 situation).

The hole type connections

$$H3: T_- \rightarrow T_+ \text{ and } T_+ \rightarrow T_-$$

may take various forms due to the different stability properties of these fixed points in different parameter regimes according to T_\pm 's. In region III of Figures 4 and 5, for instance, we might expect the $T_- \rightarrow T_+$ connection to exist continuously as the parameters are varied, due to the likely transverse intersection of two 2-manifolds in 3-space. Our numerical work for $c = 0$ supports this conjecture.

The possible connections

$$H4: D_+ \rightarrow T_\pm \text{ and } T_\pm \rightarrow D_-$$

are of particular interest in describing transitional fronts from the laminar state. Once again these may also take various forms depending on the stability properties of the fixed points.

Note that in regions IIa and IIb of parameter space the plane wave solutions T_- and T_+ are asymptotically stable and unstable respectively. We are thus motivated to seek solutions of type $H3$ and $H4$ in these regions, which, if existing at all, would exist for a continuum of parameter values. Similarly in regions Va and Vb, where the stability properties are identical.

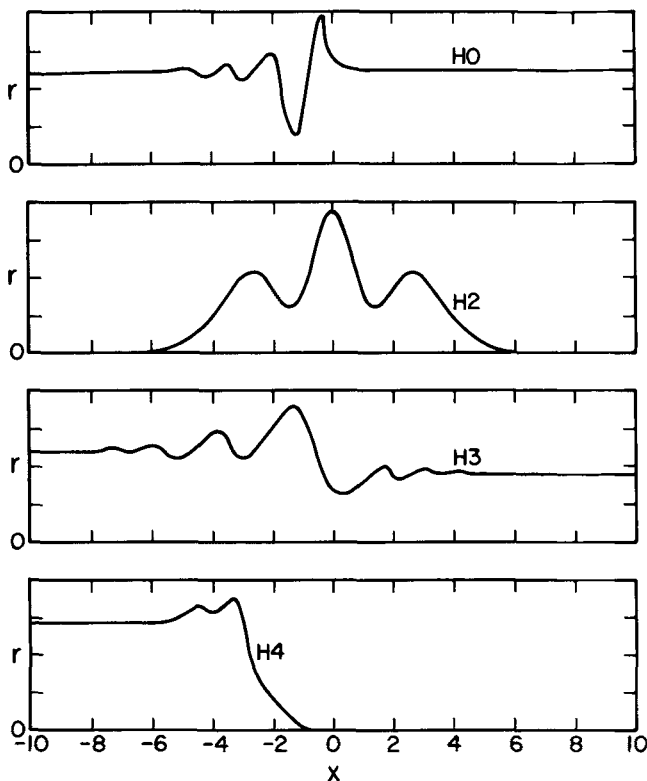


Figure 18. Modulus squared versus X for solitary wave solutions resulting from homoclinic and heteroclinic orbits of Figure 17. H_0 and H_3 are hole type solutions, H_2 a breather, and H_4 a front or shock.

In regions IVa and IVb the points D_+ and D_- are stable and unstable respectively, so that we can also seek solutions of type H_4 for those values of Ω and c . Such investigations are carried out in Section 6.3.

6.2. Some analytic solutions for solitary waves

It is somewhat surprising that three exact solutions are known which describe heteroclinic orbits for the system (4.1). It is also interesting to observe that these three solitary wave solutions are of the form of the breather, front (shock or kink), and hole solutions respectively, which arise in the study of the sine-Gordon equation. Their forms become particularly simple when cast in the framework of the reduced form of the complex Duffing equation.

The first, referenced above as the solitary wave of type H_2 , was first written down by Hocking and Stewartson as a solution of the GL equation

$$A = \lambda L e^{-i\Omega t} (\operatorname{sech} \lambda x)^{1+i\nu},$$

where the parameters in the equation are uniquely determined by the GL

coefficients. For the reduced system (4.1) this solution is of the form

$$r = \lambda^2 L^2 \operatorname{sech}^2 \lambda x, \quad w = -\lambda \tanh \lambda x, \quad s = \nu w. \quad (6.1)$$

We find that

$$\lambda^2 = \frac{\delta_1}{\nu^2 - 1}, \quad L^2 = -\frac{3\nu}{\gamma},$$

and

$$\frac{\beta}{\delta_1} = \frac{2\nu}{1 - \nu^2}.$$

In this and the other solutions to follow, ν is given by a root of the appropriate sign of the equation

$$\nu^2 + 3\nu \frac{\delta_2}{\gamma} - 2 = 0. \quad (6.2)$$

This breather solution always exists if $\delta_2 < 0$, and when $\delta_2 > 0$ it exists only for $\delta_1 > 0$. For the Poiseuille flow parameters (2.4) we must have $\sigma_r > 0$, and we find that when $\sigma_r = 1$, $\Omega = 6.058$.

This solution and another two heteroclinic orbits were found exactly by Nozaki and Bekki [19]. These authors extended to the GL equation the direct method of Hirota [7] for finding solitary wave solutions of the cubic Schrödinger equation, which is based on the fact that these partial differential equations may be written in terms of bilinear differential operators. They assumed that $\sigma_r d_r < 0$ in the GL equation, though we find that this is an unnecessary restriction.

A solution that we find most interesting has the form of a front, where the solution tends to a traveling wave at minus infinity and to zero at plus infinity. In this case, which is H4 above, the GL solution is

$$A = Le^{i[k(x-ct)-\Omega t]}[1 - \tanh \lambda(x-ct)][\operatorname{sech} \lambda(x-ct)]^{i\nu},$$

so the solution to the ordinary differential equations (4.1) is of the form

$$r = L^2(1 - \tanh \lambda X)^2, \quad s = k - \nu \lambda \tanh \lambda X, \quad w = -\lambda(1 + \tanh \lambda X).$$

On solving the six simultaneous equations which result in our 3-D representation, we get

$$\lambda^2 = \frac{\delta_1}{8-9a_0^2}, \quad L^2 = \frac{3\nu\lambda^2}{\gamma},$$

$$\frac{\beta}{\delta_1} = \frac{18a_0}{9a_0^2 - 8},$$

$$c_1 = 6\lambda, \quad k = \lambda(3a_0 + \nu).$$

This shock solution exists for a large range of GL coefficients and for unique values of Ω and c . For the Poiseuille case, on returning to the original parameters we find that σ_r must be supercritical and the solution exists for $\sigma_r = 1$, $\Omega = -0.183$, and $c = 2.14$, and thus is a heteroclinic orbit between T_+ and D_- existing in region IVa of parameter space. This solution is codimension-2, due to the coincidence of two 1-D manifolds. In this way it is a special case of the connection $H4$. Note that due to the reflection symmetry (2.14), a reverse shock also exists, but for a value of c of the opposite sign from that given above.

The hole solution found by Nozaki and Bekki is of the form

$$A = \lambda L e^{-i\Omega t} \tanh \lambda x (\operatorname{sech} \lambda x)^{i\nu}.$$

Cast in the 3-D dynamical system form we find

$$r = \lambda^2 L^2 \tanh^2 \lambda x, \quad s = -\nu \lambda \tanh \lambda x, \quad w = \frac{2\lambda}{\sinh 2\lambda x},$$

where for existence one must satisfy

$$\lambda^2 = \frac{\delta_1}{2}, \quad L^2 = \frac{3\nu}{\gamma},$$

and

$$\frac{\beta}{\delta_1} = \frac{3\nu}{2}.$$

For Poiseuille parameters we find that the hole solution exists only for supercritical σ_r , and when $\sigma_r = 1$, $\Omega = 3.45$. This solution requires the symmetry of $c = 0$ and exists for a discrete value of Ω only, as it occurs due to the coincidence of two 1-D manifolds. Notice that the solution tends to the traveling waves T_- and T_+ at plus and minus infinity and there is a singularity in w where the solution passes through amplitude zero. This solution exposes the weakness of the 3-D phase invariant formulation of the problem, in which it has a singularity of the form (4.5). The solution is analytic in the original variables, however, where in the 4-D formulation it corresponds to an orbit of odd symmetry tending to the plane wave periodic orbits at plus and minus infinity.

6.3. Numerical results

We first describe the family of symmetric breather solitary wave solutions of type $H1$ that we have found for $c = 0$. The shooting method used solves the initial-value problem in x for the reduced system from close to D_+ on the linearization of its 1-D unstable manifold and shoots to a point $(r_1, 0, w_1)$ on the Poincaré plane $s \equiv 0$. All our numerical integrations were performed using the Sandia ODE package. Newton's method with a numerical Jacobian was then used to solve $w_1(\Omega) = 0$. On Newton convergence the resulting orbit approximates half of a

symmetric breather solution at a value of Ω determined by the iteration procedure. Our method recovered the known exact solution (6.1) to greater than 6-digit accuracy. It also converges to a large number of other previously unknown breather type solutions, provided $\sigma_r > 0$. These solutions possess a discrete spectrum of frequencies for $\Omega > a_0\sigma_r$. This lower bound for Ω when $c = 0$ follows from the relation

$$\int_{-\infty}^{\infty} r(\gamma r - \beta) dx = rs|_{-\infty}^{\infty},$$

which is derived from the dynamical equations (4.1) by integration by parts. The boundary term vanishes on a breather solution, and thus β must be positive for such a solution to exist. Although we cannot prove the existence of these other heteroclinic orbits in the (r, s, w) phase space, we believe the numerical evidence for their existence is very strong.

In our shooting method we may choose the number of times n_s the orbit is to pass through the $s \equiv 0$ Poincaré plane before hitting the r -axis. When $n_s = 0$ we converged to 10 breather type solutions, the number limited by the set of initial Ω -values in the Newton procedure. Two breather solutions found with $n_s = 0$ are shown in Figure 19(a) and (b). Similarly we find more breather type solutions with $n_s \geq 1$, two of which are plotted in Figure 19(c) and (d). No solutions were found for $\sigma_r < 0$.

We expect that an infinite number of breathers exist, each one the infinite period limit of a branch of periodic orbits. This is based on our conjecture that an infinite number of periodic branches bifurcate from the branch $P0$ which behave similarly to $Q1$, $Q2$, $Q4$, and $Q5$ of Figure 8. All of these solitary waves are steady in the group velocity frame for Poiseuille flow but have distinct temporal frequencies of oscillation.

Our attempts to find nonsymmetric solitary waves decaying at plus and minus infinity were unsuccessful. We used a Newton procedure in which shooting was performed from the 1-D unstable and stable manifolds of D_+ and D_- respectively to the plane $w \equiv 0$. Both c and Ω were shooting parameters, and there was no convergence except to the symmetric breathers when $c = 0$.

We also know from continuing the branch $P1$ in the 4-D phase space that at least one breather solution exists which has the odd symmetry, which is singular in the reduced representation. Again we might expect a discrete spectrum of these solutions in Ω for $c = 0$. Similarly the continuation of branch $Q3$ suggests that at least one pair of hole type solutions $H3$ exists for a discrete spectrum of Ω and $c = 0$.

The heteroclinic connection $H3$ joining the plane waves T_{\pm} is known to exist for $c = 0$ when the two fixed points are “close” to where they coalesce and disappear in a saddle-node bifurcation. Kopell and Howard [14] have some general results on the existence of this connection when the distance between T_+ and T_- is small, and P. Holmes [12] has a similar result for small β and γ . We have numerical results that suggest that this symmetric connection persists for varying Ω whenever the plane wave fixed points exist (and $c = 0$), and occurs due to the intersection of two 2-D invariant manifolds in 3-space. Again we used a

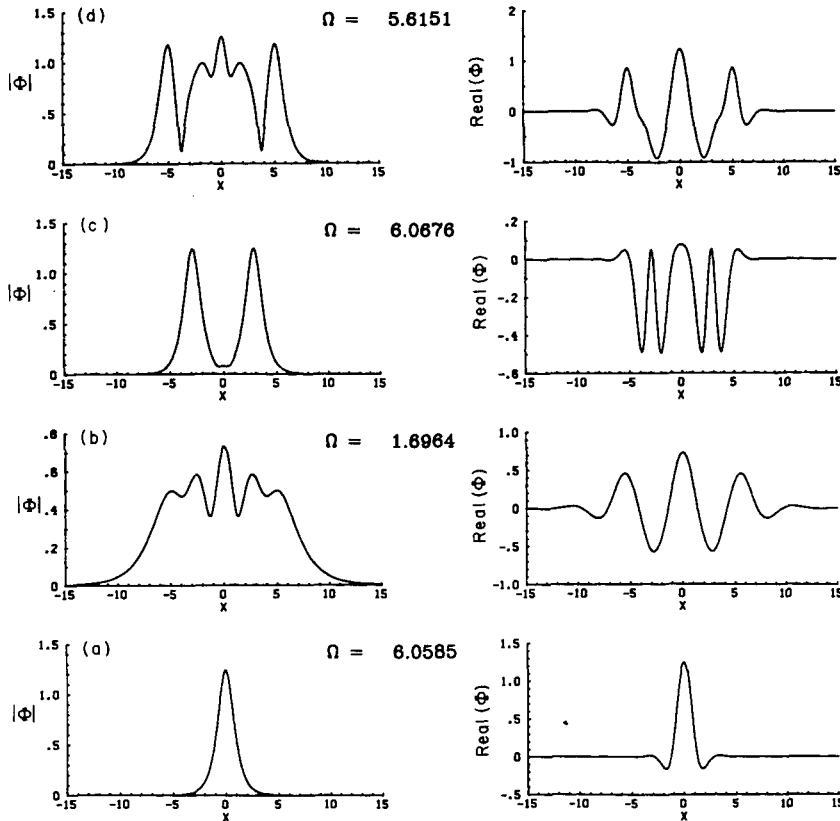


Figure 19. Real part and modulus of some breathers which exist for $c = 0$ and $\sigma_r = 1$. (a) is the exact solution (6.1) which is the infinite period limit of branch $Q1$.

Newton-Poincaré plane method to shoot from the point T_- to get to a point on the r -axis in phase space. The initial condition was chosen on an arbitrarily small circle about T_- lying in its planar unstable eigenspace, the shooting parameter being the position of the initial condition on this circle. In this way a family of symmetric hole type solitary waves was found to exist connecting the distinct plane wave solutions either side of the critical value of $\sigma_r = 0$. We also expect these solutions to exist as c is perturbed from 0 provided the plane wave fixed points remain as saddle points in phase space (i.e. in region III of phase space). Such nonsymmetric heteroclinic orbits would thus connect plane waves of different amplitudes, as illustrated in $H3$ of Figure 18.

We now discuss a class of solitary-wave-type solutions describing a transition from the laminar state or plane wave states. These solutions have the common feature that they exist for nonzero c and are structurally stable in that they persist under perturbations in both Ω and c . This is because the orbit in the reduced phase space corresponding to each solution approaches a stable attractor as $X \rightarrow \infty$, or by symmetry a repellor as $X \rightarrow -\infty$. In what follows our remarks will refer only to solutions with $c > 0$, recalling that to each such solution there

corresponds a reflected quasisteady solution of the GL equation with speed correction $-c$.

We are interested in determining orbits which lie in the basins of attraction of any bounded attractors. We shoot from a given initial condition in the (r, s, w) phase space and observe whether the trajectory approaches a bounded attractor. In all cases when this did not occur, the trajectory tended to amplitude infinity, becoming spatially unbounded for a finite value of X , and thus not of interest here. As we are concerned with solutions on the infinite interval, the initial conditions were chosen on the unstable manifolds of the fixed points D_{\pm} and T_{\pm} provided they exist.

From our discussions so far, there are two main sectors of parameter space to search. When $\sigma_r > 0$ we seek solutions in region IVa tending to D_+ as $X \rightarrow \infty$, the only possible initial condition of the above type being on the 1-D unstable manifold of T_+ . The second case occurs for σ_r of either sign, when there can exist stable attractors in regions IIa, Va and III. In IIa (and similarly Va for $\sigma_r > 0$) the fixed point T_- is stable, and in region III there is at least one family of periodic orbits which are stable. We find that there is also the possibility of a strange attractor in this region of parameter space, as we describe below. In regions IIa, III, and Va we can shoot from the 1-D unstable manifolds of either T_+ or D_+ . In addition, in region III we can also shoot from the 2-D unstable manifold of T_- .

Our numerical computations of frontlike solutions of type $H4$ ($T_+ \rightarrow D_+$) when $\sigma_r > 0$ suggest that these solutions exist for all values of the parameters Ω and c in region IVa. Two such solutions are shown in Figure 20, where we display both the modulus and the real part of the solution $\Phi(X)$ reconstructed from (r, s, w) via the transformation (2.10). Such frontlike solutions can exist

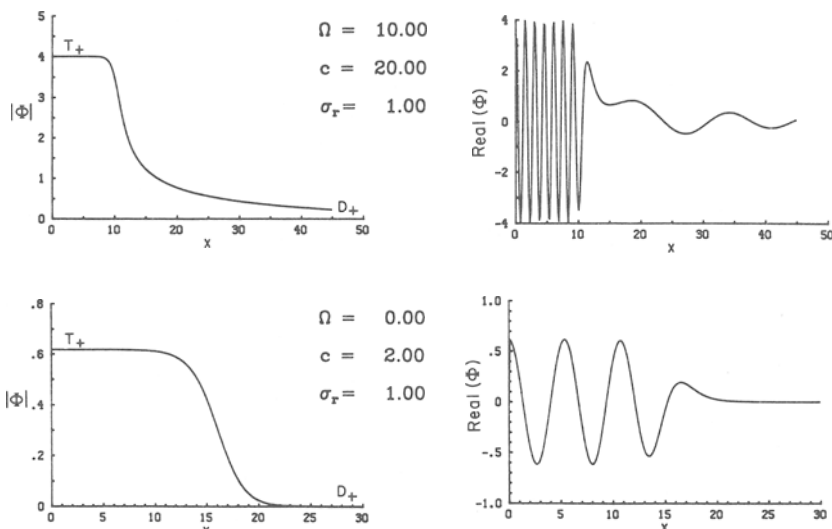


Figure 20. Front solutions ($T_+ \rightarrow D_+$) with $c > 0$ in region IVa of parameter space, existing only for $\sigma_r > 0$.

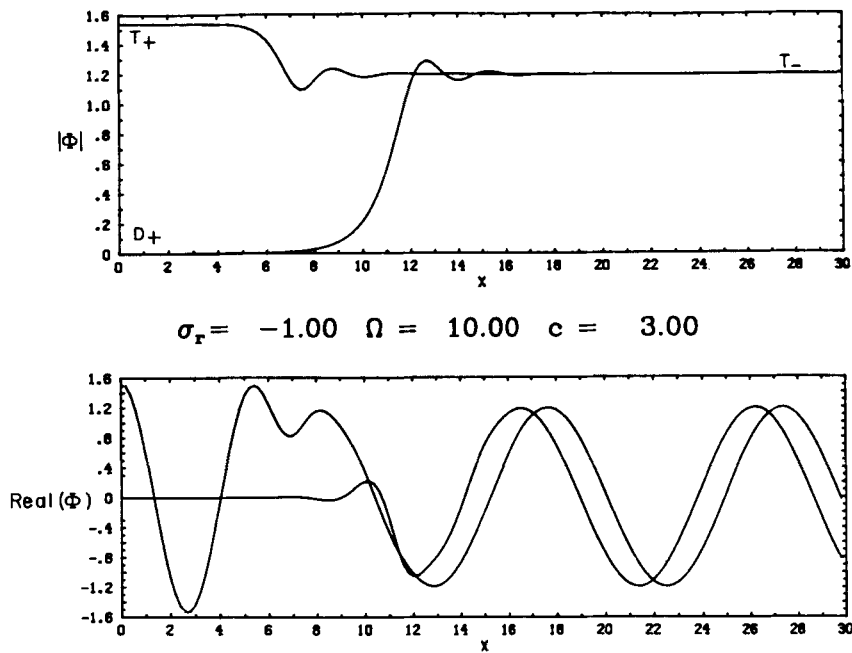


Figure 21. Real part and modulus of hole and front solutions in region IIa for $\sigma_r < 0$.

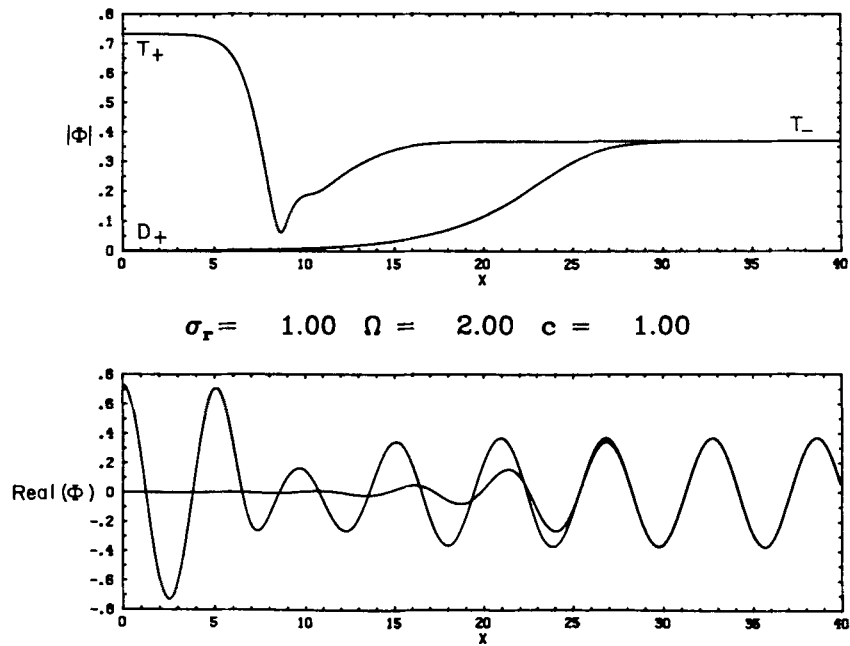


Figure 22. Real part and modulus of hole and front solutions in region IIa for $\sigma_r > 0$.

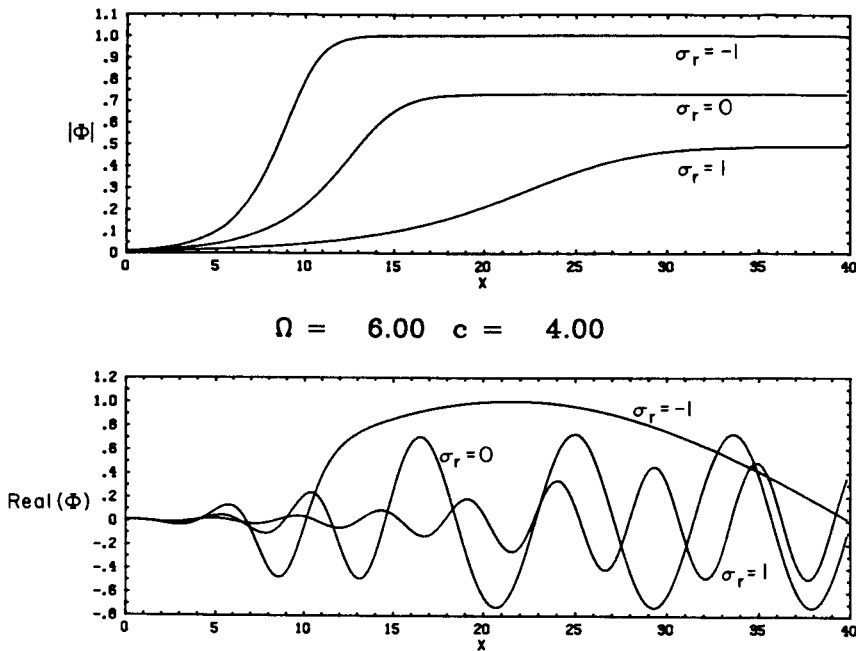


Figure 23. Front solutions ($D_+ \rightarrow T_-$) for σ_r either side of critical for fixed Ω and c .

with a positive speed correction c only for supercritical Reynolds numbers ($\sigma_r > 0$).

In region IIa (and similarly Va) the plane wave solution T_- is spatially stable. Figures 21 and 22 illustrate that hole H3 ($T_+ \rightarrow T_-$) and front H4 ($D_+ \rightarrow T_-$) solutions exist for σ_r either sign. Figure 23 also shows a series of front solutions with Ω and c fixed and σ_r varying between sub- and supercritical Reynolds numbers. As far as we can tell from a limited search of parameter space, these two types of heteroclinic orbits exist for a large proportion of regions II and V, although the unstable manifold of D_+ is sometimes found to be spatially unbounded. The hole and front solutions in region Va which we have found are similar to those shown in Figure 22, although their spatial scale is much larger and the phase oscillates rapidly due to the larger values of the coordinate s involved.

In region III there are no stable fixed points; however, from our numerical work of Section 5 we know that there exist attracting periodic orbits in the reduced phase space corresponding to 2-tori for the complex amplitude. The dynamics in phase space for this sector of parameter space seems extremely complex, and our studies are limited. Here we describe some of the behavior for $\sigma_r = 1$, $\Omega = 2$ fixed and varying $0 < c < 0.515$, which is the value at which T_- loses stability in a supercritical Hopf bifurcation. Recall that the periodic orbit on branch C2 shed in this bifurcation (see Figure 12) is stable until it undergoes a series of period doublings as c is decreased. Figure 24 shows the modified front and hole solutions at $c = 0.3$, where this periodic orbit is stable, which result from

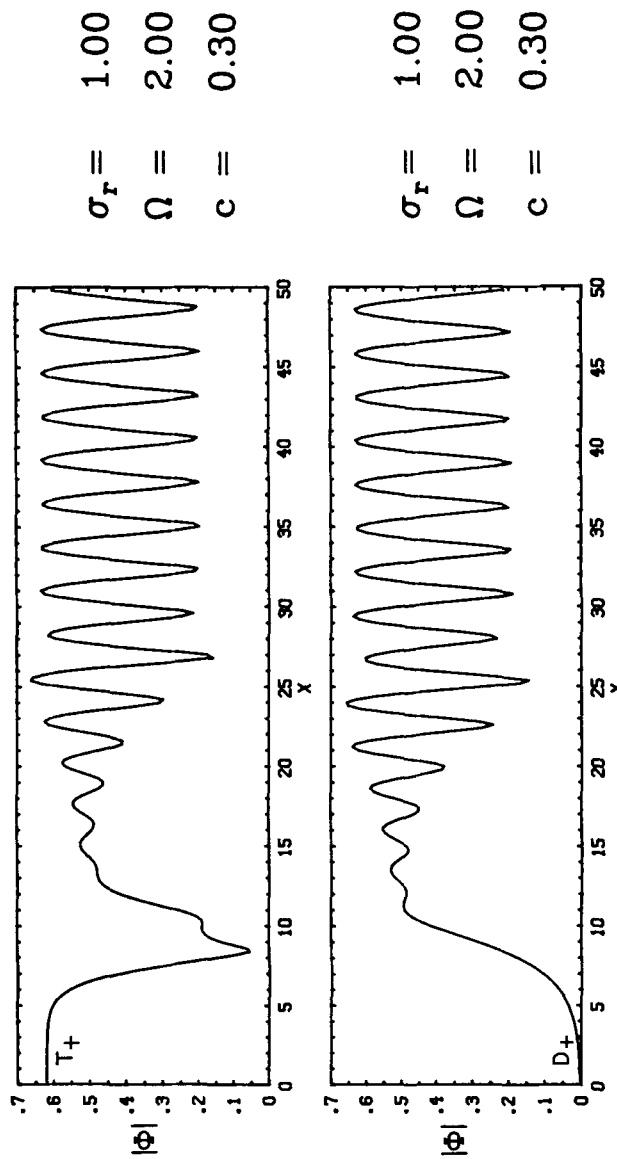


Figure 24. Transition from plane wave (a) and laminar solution (b) in region III to the stable periodic orbit on branch C2.

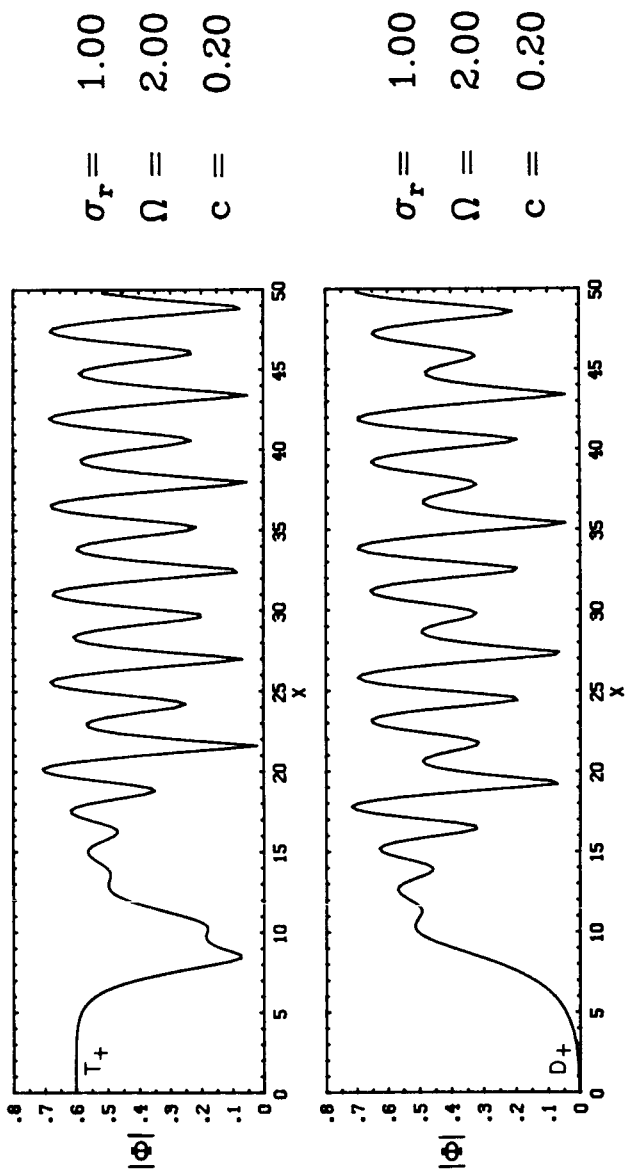


Figure 25. Transition from plane wave (a) and laminar solution (b) in region III to distinct periodic orbits. (a) approaches the period doubled branch $C3$, and (b) approaches a previously undiscovered stable orbit.

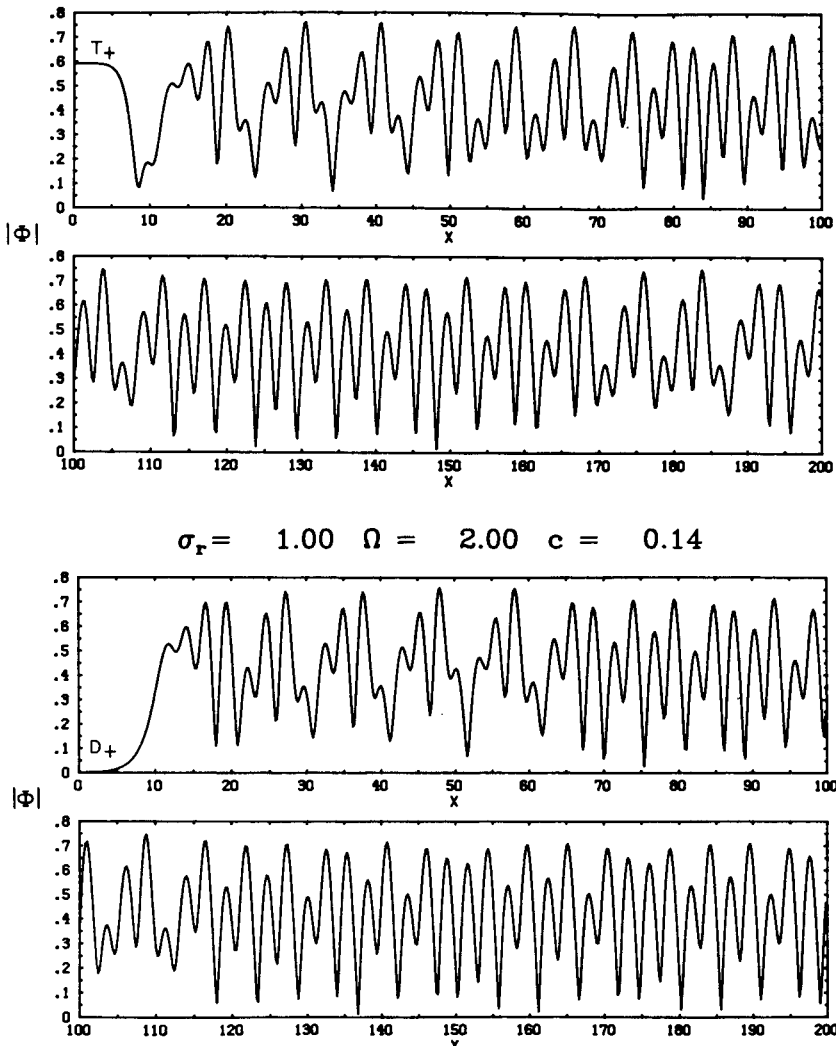


Figure 26. Transition from plane wave (a) and laminar solution (b) in region III to apparently nonperiodic states, $\sigma_r > 0$.

shooting from D_+ and T_+ respectively. Similar behavior results from shooting from T_- , although there is a one parameter family of solutions attracted to $C2$ from this plane wave, as this fixed point is 2-dimensionally unstable. When $c = 0.2$ the unstable manifold of T_+ is attracted to the period doubled orbit on $C3$ as shown in Figure 25. However, a nonuniqueness is seen to arise as the front solution emanating from D_+ is attracted to a different periodic orbit.

Decreasing c further, we find attractors of higher period and perhaps chaotic attractors. In Figure 26 we show the pair of solutions from D_+ and T_+ for $c = 0.14$. By inspection of these and other orbits for c in a neighborhood of this

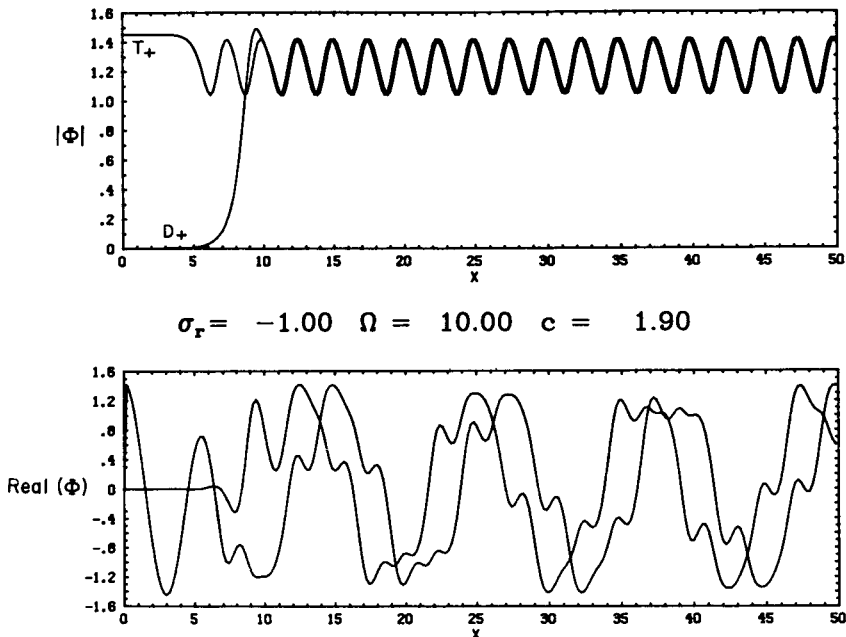


Figure 27. Transition from plane wave (a) and laminar solution (b) to a quasi-periodic solution in region III for $\sigma_r < 0$.

value, it appears that these solutions are nonperiodic. It is possible that they are very long transients to a periodic or quasiperiodic state, or chaotic. In any case they illustrate a transition from the laminar and plane wave solutions to a finite amplitude spatially complicated state. Lastly, for $\Omega = 2$ and c less than about 0.1 the orbits from D_+ and T_{\pm} become spatially unbounded.

When shooting from these three fixed points in region III for $\sigma_r = -1$, only the periodic branch $C0$ of Figure 7, corresponding to spatially quasiperiodic solutions of the GL equation, is found to be attracting. Recall that such solutions which bifurcate from T_- do not appear to undergo period doubling bifurcations as is possible when $\sigma_r > 0$. Figure 27 illustrates the modulus of the amplitude of the unstable manifolds of D_+ and T_+ for one set of parameters in this region where such a periodic orbit is attracting. From our limited numerical search we find that for fixed Ω the unstable manifolds become unbounded before the periodic branch becomes homoclinic as c is decreased. We have been unable to find any other more complex bounded behavior for subcritical σ_r .

7. Application to shear flows

We believe that the existence of the quasisteady solutions of the Ginzburg-Landau equation described above may be relevant to the study of transition in shear flows. In this final section we give evidence to this effect and hypothesize the existence of solutions of the Navier-Stokes equations which have the features of transition from the laminar state.

7.1. The validity of the GL equation

The GL equation describes the evolution of modulations to the primary linear wave of instability for Poiseuille flow at Reynolds numbers near critical. The Stewartson-Stuart derivation of the GL equation will also apply to other flows for which there is a neutral curve of Orr-Sommerfeld type, and in this sense the GL equation is the generic amplitude equation for fluid problems where a continuum of wavenumbers becomes unstable as the control parameter is increased above a finite threshold.

In order to determine whether the features of the GL equation carry over to the Navier-Stokes equations, one must assess the structural stability of this truncation of the full equations and also its region of validity. This is a difficult question to address and arises whenever an approximation to the full physical model occurs. Presently all we are able to say is that the large class of quasisteady solutions which we have found will persist under perturbations to the coefficients of the GL equation. This property is essential, as we have used values of these coefficients that are approximate, coming from numerical calculation. In addition, the small magnitude of s , in the definition of ϵ (1.5) may allow the GL equation to have a relatively large range of validity in amplitude and Reynolds number.

Another question that we have so far not addressed is that of the choice of initial and boundary conditions for the GL equation. The derivation by Stewartson and Stuart [22] assumes an infinitesimal localized initial condition which initially develops according to linear theory. This leads to localization in space for all finite time, and thus the correctly posed boundary conditions for the GL equation are

$$|A| \rightarrow 0 \quad \text{as } x \rightarrow \pm \infty. \quad (7.1)$$

This approach was taken to ensure that a self-consistent rational theory resulted. With an infinitesimal initial condition, for any fixed $\text{Re} < \text{Re}_c$ the solution will decay to the laminar state, as the effect of the destabilizing nonlinearity of the GL equation will remain negligible. This issue is discussed by Hocking et al. [9], and we agree with their conclusion that the GL equation contains the structure of the subcritical instability, which is only revealed if finite amplitude GL solutions are considered. In this way we must relax Stewartson and Stuart's original assumptions in order to allow finite amplitude states for $\text{Re} < \text{Re}_c$. Similarly we have relaxed the condition (7.1) on almost all of the solutions we have discussed in this paper, with the exception of the breather solutions decaying at infinity. In our study of quasisteady states it is only reasonable to allow the most general boundary condition possible,

$$|A| < K \quad \text{for all } x,$$

as we have been studying the structure of the GL equation independent of the evolution of initial conditions. Most often we have found $|A|$ approaches a steady state at plus or minus infinity or is periodic for all x .

Numerical eigenvalue calculations for the stability of spatially periodic quasisteady solutions for sub- and supercritical values of σ , (and $c = 0$) suggest that all of these solutions are temporally unstable [15]. This is in agreement with numerical calculations for the time dependent equations. Our experience in solving the initial value problem for the GL equation relevant to Poiseuille flow with periodic boundary conditions is that solutions become unbounded in finite time because the nonlinear term is unable to cause amplitude saturation as it does when the real part of the nonlinearity is negative. In contrast, Hocking and Stewartson [8] solved the initial value problem with zero end conditions on a finite domain, and their computations revealed solutions that remained bounded but appeared irregular in space and time.

In any case there are several motivations for studying the quasisteady GL equation, whose solutions are temporally unstable. The first is that the continuation of an unstable branch of solutions may lead to its stabilization at different parameter values. The canonical example for this is the existence of the plane waves T_{\pm} in the GL equation. These give the existence for small amplitude of the equilibrium branch of traveling waves for Poiseuille flow described in Section 2, which although unstable for both the GL and Navier-Stokes equations at small amplitude, becomes stable to a general class of perturbations at large amplitude at Reynolds numbers far less than Re_c of linear theory. In this way we might expect other branches of solutions suggested by the GL equation for Poiseuille flow to have continuations down to lower Re , where we seek to find solutions indicative of the experimentally observed subcritical threshold [18]. Secondly, the knowledge of the structure of steady solutions of a differential equation often lends insight into the dynamics of the time dependent problem. Moreover, with the use of dynamic control a physically desirable steady state can be attained which otherwise could never be observed without external forcing.

The many quasisteady solutions that we have found for the GL equation derived for plane Poiseuille flow are often nonunique and exist for either a discrete or a continuous spectrum of the two undetermined parameters Ω and c , the temporal frequency and wave speed correction to the group velocity of linear theory. This degeneracy often arises in parabolic problems where the wave speed is left undetermined. Hence, if these periodic solutions are relevant to the unsteady Poiseuille problem, one may hope to find an underlying selection mechanism so that only a few of the solutions are realized in the initial value problem.

7.2. Interpretation of the quasisteady solutions

Given that the above scenario holds and that the solutions for the Ginzburg-Landau equation that we have found are in direct correspondence with solutions of the Navier-Stokes equations, the periodic and quasiperiodic GL solutions seem to describe quasiperiodic packets of instability. A large range of solutions exists for both sub- and supercritical Reynolds numbers, whose modulating envelopes possess different temporal frequencies of oscillation and varying speeds about the group velocity of linear theory. Such weakly nonlinear modulations to the Tollmien-Schlichting waves have been observed in the pioneering experiments of

Schubauer and Skramstad [10] in their study of laminar boundary layer transition. These slow modulations appear downstream of the leading edge of the flat plate and persist until 3-D bursts develop. For plane Poiseuille flow experimental work is far more difficult and incomplete than for boundary layers, and it is less clear what the secondary processes of transition from the initial growth of TS waves are, although it appears that the onset of 3-D effects occurs much sooner than in the boundary layer [18].

The periodic envelope solutions are also reminiscent of the slugs and puffs of instability that divide sections of laminar flow in pipe flow. We cannot dwell on this similarity, as it is accepted that there is no point of linear instability for circular pipe flow, and thus it is not clear that one can derive an equation of GL type for this flow. However, in circular pipe flow, if the laminar solution is perturbed sufficiently, there appears to exist a subcritical instability to a finite amplitude state. It is therefore possible that the structure of the GL equation, in allowing the description of finite amplitude periodic and quasiperiodic solutions for $\sigma_r < 0$, in some way models these subcritical states.

The solitary wave solutions of the GL equation and their generalizations which correspond to stable and unstable manifolds in phase space are of particular interest because we know that the four fixed points in the reduced phase space we have studied correspond with known solutions of the full 2-D Navier-Stokes equations.

The breather-type solutions are a class of solutions where the envelope of the TS waves is localized so that the flow is laminar both up and downstream. We expect that there is an infinite number of these solutions moving at the group velocity with a given discrete set of temporal frequencies. These solutions arise as the limiting cases of the periodic solutions when the wavelength tends to infinity.

The front solutions describe a sharp transition between laminar flow and a plane wave and are found to exist at a given Reynolds number for a continuous spectrum of frequency and speed. A front from wavelike to laminar behavior traveling faster than the group velocity ($c > 0$) exists only for supercritical Reynolds numbers ($\sigma_r > 0$). Similarly, by symmetry, there will also exist a transition from the laminar to the wavelike state traveling slower than the group velocity. See Figure 28. If we think of these solutions as approximating the front and rear sections of a fully time dependent section of instability, these results suggest that in a neighborhood of critical, the instability can spread only for $Re > Re_c$, but can decay for Re either side of Re_c .

The solutions connecting plane waves of the same or different wavenumber which can exist for a continuum of temporal frequencies or speeds are more difficult to interpret. These, however, are quite likely to exist in the full fluid equations as connecting solutions between the well-established finite amplitude steady waves.

Lastly we have found transition solutions described by the unstable manifolds of the plane waves and laminar state in region III of parameter space either side of critical. The transition from undisturbed flow to a more complex finite amplitude state which is quasiperiodic or perhaps chaotic in the moving frame is of particular interest. The former were found to exist for σ_r , either side of critical; the latter for a supercritical value only. These finite amplitude quasisteady states

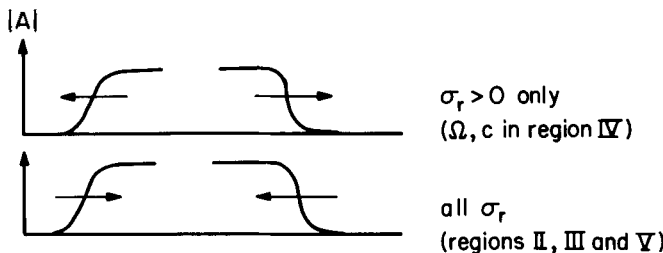


Figure 28. Diagram illustrating that the velocity of front solutions is positive in the group velocity frame only for supercritical σ_r .

are in need of further investigation both in the context of the GL equation and in that of plane Poiseuille flow.

7.3. Final remarks

Any reasonably complete theory of laminar-turbulent transition must be able to describe the 3-D structures that are observed in shear flows. Studying 2-D models such as that of the GL equation is not irrelevant, however, as experimentally there are many stages in transition, the first of which appears to retain the 2-dimensionality of the base flow, in accordance with Squire's theorem for parallel shear flows [4]. We point out the existence of a 3-D generalization of the GL equation derived for plane Poiseuille flow by Davey, Hocking, and Stewartson [1], which consists of the 3-D analogue of the GL equation coupled with an elliptic equation for the spanwise pressure gradient. It may be possible to find fully 3-D quasisteady structures for this equation, and some work on plane wave stability has recently been carried out by C. Holmes [11].

Our next aim is to be able to find quasisteady solutions to the equations of 2-D plane Poiseuille flow that are continuations of those found for the GL equation. The existence of multiple scales in both space and time suggests that the straightforward Galerkin and collocation methods used to find the equilibrium traveling wave solutions would render the discretized problem prohibitively large even on current supercomputers. In the future we hope to report on the application of other approximate methods to the 2-D Navier-Stokes equations to find these fronts and periodic structures.

Acknowledgments

I would like to express my gratitude to Professor P. G. Saffman for his valuable advice and encouragement. Thanks also go to Dr. P. Blennerhassett for helpful discussions, and Professor E. Doedel for use of and assistance with the AUTO software.

This work was supported by the Office of Naval Research (N00014-85-K-0205).

References

1. A. DAVEY, L. M. HOCKING, and K. STEWARTSON, On the nonlinear evolution of three-dimensional disturbances in plane Poiseuille flow, *J. Fluid Mech.* 63:529–536 (1974).
2. R. J. DEISSLER, Noise-sustained structure, intermittency, and the Ginzburg-Landau equation, *J. Statist. Phys.* 40:371–395 (1985).
3. E. J. DOEDEL and J. P. KERNEVEZ, Software for continuation and bifurcation problems in ordinary differential equations with applications, Applied math. technical report Caltech. (1986).
4. P. G. DRAZIN and W. H. REID, *Hydrodynamic Stability*, Cambridge U.P., 1981.
5. M. GOLubitsky and I. STEWART, Hopf bifurcation in the presence of symmetry, *Arch. Rational Mech. Anal.* 87:107–165 (1985).
6. T. HERBERT, Stability of plane Poiseuille flow—theory and experiment, *Fluid Dynamics Trans.* 11:77–126 (1981).
7. R. HIROTA, Direct method of finding exact solutions of nonlinear evolution equations, *Bäcklund Transformations* (R. M. Miura, Ed.), Lecture Notes in Math, Vol. 515, Springer, 1976, pp. 40–68.
8. L. M. HOCKING and K. STEWARTSON, On the nonlinear response of a marginally unstable parallel flow to a two-dimensional disturbance, *Proc. Roy. Soc. London Ser. A* 326:289–313 (1972).
9. L. M. HOCKING, K. STEWARTSON, and J. T. STUART, A nonlinear instability burst in plane parallel flow, *J. Fluid Mech.* 51:705–735 (1972).
10. C. A. HOLMES and D. WOOD, Studies of a complex Duffing equation in nonlinear waves on plane Poiseuille flow, preprint, Imperial College, London.
11. C. A. HOLMES, Bounded solutions of the nonlinear parabolic amplitude equation for plane Poiseuille flow, *Proc. Roy. Soc. London Ser. A* 402:299–322 (1985).
12. P. HOLMES, Spatial structure of time-periodic solutions of the Ginzburg-Landau equation, *Physica* 23D: 84–90 (1986).
13. L. R. KEEFE, Dynamics of perturbed wavetrain solutions to the Ginzburg-Landau equation, *Stud. Appl. Math.* 73:91–153 (1985).
14. N. KOPELL and L. N. HOWARD, Target patterns and horseshoes from a perturbed central-force problem: Some temporally periodic solutions to reaction diffusion equations, *Stud. Appl. Math.* 64:1–56 (1981).
15. M. J. LANDMAN, Ph. D. Thesis, California Institute of Technology, (1987).
16. H. T. MOON, P. HUERRE, and L. G. REDEKOPP, Transitions to chaos in the Ginzburg-Landau equation, *Physica* 7D:135–150 (1983).
17. A. C. NEWELL and J. A. WHITEHEAD, Finite bandwidth, finite amplitude convection, *J. Fluid Mech.* 38:279–303 (1969).
18. M. NISHIOKA, Laminar-turbulent transition in plane Poiseuille flow, in *Recent Studies on Turbulent Phenomena* 1985, pp. 193–203.
19. K. NOZAKI and N. BEKKI, Exact solutions of the generalized Ginzburg-Landau equation, *J. Phys. Soc. Japan* 53(5):1581–1582 (1984).
20. G. G. SCHUBAUER and H. K. SKRAMSTAD, Laminar boundary-layer oscillations and stability of laminar flow, *J. Aero. Sci.* 14:69–78 (1947).
21. L. SIROVICH and P. K. NEWTON, Periodic solutions of the Ginzburg-Landau equation, *Physica* 21D: 115–125 (1986).
22. K. STEWARTSON and J. T. STUART, A non-linear instability theory for a wave system in plane Poiseuille flow, *J. Fluid Mech.* 48:529–545 (1971).
23. J.-P. ZAHN, J. TOOMRE, E. A. SPIEGEL, and D. O. GOUGH, Nonlinear cellular motions in Poiseuille channel flow, *J. Fluid Mech.* 64:319–345.

CALIFORNIA INSTITUTE OF TECHNOLOGY

(Received October 10, 1986)